Quaternary Science Advances 23 (2026) 100333

Contents lists available at ScienceDirect

Quaternary Science Advances

journal homepage: www.sciencedirect.com/journal/quaternary-science-advances

Abundance and morphology of microscopic charcoal in modern marine sediments to refine the interpretation of paleofire records in the Western Mediterranean region

Marion Genet [a,b,*], Anne-Laure Daniau [a,**], Florent Mouillot [c], Sabine Schmidt [a], Bernard Dennielou [d], Serge Berné [e], Vincent Hanquiez [a], Mostefa E. Kouachi [c,f], Muriel Georget [a]

[a] University Bordeaux, CNRS, Bordeaux INP, EPOC, UMR 5805, Pessac, F-33600, France
[b] Geo-Ocean, Univ Bretagne Sud, Univ Brest, CNRS, Ifremer, UMR6538, Vannes, F-56000, France
[c] UMR CEFE, Univ. Montpellier, CNRS, EPHE, IRD, 1919 route de Mende, 34293, Montpellier, CEDEX 5, France
[d] Ifremer, Unité Géosciences Marines, Centre Bretagne, Plouzané, 29280, France
[e] CEFREM UMR5110 CNRS, Université de Perpignan Via Domitia, Perpignan, France
[f] Forests Conservation of Sétif, Directorate General of Forests (DGF), Cité Ain Tbinet, Sétif, 19000, Algeria

A R T I C L E I N F O

Keywords:
Biomass burning
Remote sensing
Fire regime
Climate
Vegetation

A B S T R A C T

Paleofire records represent a valuable resource for understanding long-term changes in biomass burning and fire activity, as well as their drivers. Furthermore, they offer a way to assess fire models under climatic conditions that differ from those prevalent in the contemporary era. However, further calibration studies are needed to refine the link between paleofire records and more detailed characteristics of paleofire regimes. In order to enhance our understanding of the charcoal proxy, we analysed microscopic charcoal abundance and morphology in 277 marine surface sediment samples from the eastern Atlantic Ocean off the Iberian Peninsula and the western Mediterranean Sea, and investigated their link with fire regime characteristics, climate and fuel over adjacent land in the Western Mediterranean region. Our results show that squared microscopic charcoal particles are correlated with forest fires, while elongated microscopic charcoal particles are associated with the combustion of open and mixed vegetation, so that tree *vs* grass burning can be inferred by the relative changes in mean microscopic charcoal elongation ratios. Microscopic charcoal concentrations are a function of fuel type, climate, fire frequency and burned areas.

1. Introduction

Fire is one of the main causes of environmental disruption on Earth (Bowman et al., 2009a). Increases in fire intensity could significantly impact carbon stocks ((Bowman et al., 2009), greenhouse gas emissions (Barbosa et al., 2025; Zhao et al., 2025), ecological values (Arrogante-Funes et al., 2024) and human valuable resources and infrastructures (Chuvieco et al., 2023).Such changes may also reduce ecosystem services (Lecina-Diaz et al., 2021), in particular under higher emission scenarios (Sayedi et al., 2024). Within Europe, the Mediterranean region is the main hotspot of fire activity (San-Miguel-Ayanz et al., 2023), where warmer and drier climate future climate condition are projected to substantially increase fire hazard (Moriondo et al., 2006; Mouillot et al., 2002; Ruffault et al., 2020). The probability of extremely large wildfires (>2500 ha) is expected to increase by the end of the century driven by increasing temperatures and declining relative humidity (Grünig et al., 2023). However, fire projections remain highly uncertain, as most predictive models rely on processes or statistical relationships inferred from contemporary global remote sensing data (Mouillot et al., 2014) or recent historical fire records (Gincheva et al., 2024; Mouillot and Field, 2005), and have rarely been validated beyond this period (Hantson et al., 2016). Statistical (Haas et al., 2022; Batllori et al., 2013; Forkel et al., 2019; Forrest et al., 2024; Ruffault et al., 2020), or more recently AI driven models (McNorton, 2025; Zhang

* Corresponding author. Geo-Univ Bretagne Sud Univ Brest CNRS Ifremer UMR6538 Vannes F-56000 France.
** Corresponding author. University Bordeaux, CNRS, Bordeaux INP, EPOC, UMR 5805, Pessac, F-33600, France.
E-mail addresses: marion.genet17@gmail.com (M. Genet), anne-laure.daniau@u-bordeaux.fr (A.-L. Daniau).

https://doi.org/10.1016/j.qsa.2026.100333
Received 6 February 2026; Received in revised form 6 June 2026; Accepted 11 June 2026
Available online 17 June 2026

et al., 2023) do not account for potential changes in the interactions between climate, vegetation and fires beyond modern observations. More process-based fire models can be embedded in vegetation models (see Rabin et al. (2017) for a review), but they also lack robustness in process identification and long-term benchmarking (Kloster et al., 2010; Yue et al., 2015). Using paleofire records to test these models under climatic conditions that differ from those of today's, particularly within a range comparable to future projections, can provide insights into whether models with lower performance under current conditions may exhibit greater robustness across time and climate divergence (Van der Meersch et al., 2025).

Marine sedimentary records hosting microscopic charcoals residues provide long and continuous archives of particulate matter emitted from fires under various past climatic conditions (Beaufort et al., 2003; Daniau et al., 2007, 2009, 2023). However, converting this sedimentary archives into burned biomass or fire regime characteristics such as burned area, intensity, frequency, severity or seasonality of fires (Krebs et al., 2010) remains subjected to interpretation because it is difficult to determine the role of the parameters influencing fire regime characteristics, such as climate and vegetation, and to distinguish variable actually recorded in charcoal accumulation. Furthermore the transport processes (winds, runoff, rivers, ocean currents), as well as depositional processes introduce additional uncertainty in the marine sedimentary record of microscopic charcoal, making their interpretation particularly challenging. In this respect, improving confidence in marine sedimentary charcoal as a robust reliable proxy for past fire regimes requires, further investigations of the relationships between microscopic charcoal in modern marine sediments, fire regimes and exposed vegetation. Microscopic charcoal in modern sediments off the coasts of Iberia and Africa have proven to be a reliable indicator of fire regimes and of the type of burned vegetation in adjacent watersheds (Genet et al., 2021; Haliuc et al.,2023). These two studies revealed relative changes in the mean length-to-width ratio determined the type of burned fuel. Among the different characteristics of fire regimes, fire intensity and size appears to be the most important drivers of charcoal morphotypes and abundance. In addition, charcoal abundance is potentially influenced by climatic gradients (Genet et al., 2021). Off Iberia, rare and large summer fires of high intensity spreading into open (shrub) vegetation under a hot and dry climate were detected in ocean sediments by a large amount of elongated particles, whereas low amount of squared-particle characterized small and low intensity fires spreading under a cool and wet climate (Genet et al., 2021). Off Africa, high amounts of elongated charcoal track intense and large fires spreading into open grassland-savanna vegetation, while low amounts of squared charcoal indicate small fires of low intensity, spreading in tree-dominated ecosystems (Haliuc et al., 2023).

Here, we question the spatial stability of these findings and regional comparability of the interpretation of marine sedimentary charcoal with regard to the following constraints: i) different fuel types produce different amount of charcoal and morphology (Umbanhowar. and Mcgrath, 1998), ii) different fire regime characteristics are inferred from paleofire records, iii) land use and socio-economic aspects affect fire regimes and charcoal particle emissions.

The western Mediterranean basin offers a relevant study case covering the eastern Atlantic Ocean to the western Mediterranean sea with i) contrasted temperate and Mediterranean climates, along with ii) fire occurrences driven by drought events (Turco et al., 2018) and heat waves (Ruffault et al., 2020) or strong storm activity (Pugnet et al., 2010), iii) distinct vegetation types ranging from Atlantic and Mediterranean forests to maquis and garrigue and iii) contrasted socio-economic land use (Chergui et al., 2018). To reach this goal, we build on the work of Genet et al. (2021) off the Iberian Peninsula and leverage new sediment samples collected off southeastern France, western Italy, North Africa, and the island of Mallorca to assess the abundance and morphology of microscopic charcoal. These data are then, compared with present-day fire regime characteristics, burned vegetation types, and climate conditions. This approach allows for the consideration of a greater diversity of fire regimes, vegetation types, and climatic variations, as it integrates data from different geographic regions and varied ecological contexts.

2. Present-day climate, vegetation, fire and socio-economic changes

Mediterranean ecosystems are mostly composed of forests and open woodlands (dominated by pines and evergreen oaks), or dense shrublands (dominated by woody species), and open scrublands (dominated by shrubs and grasses) (Pausas, 1999), growing under a summer-dry climate and leading to recurrent fires. At the interface between temperate and arid climates, the western Mediterranean basin then hosts more wetter sub-humid conditions at its northern bound and semi-arid conditions at its southern bound. This climate gradient influences seasonal variations in vegetation moisture content and in turn flammability (i.e the ease with which a material ignites), as well as fuel structure (quantity and connectivity) (Pausas et al., 2017; Pausas and Paula, 2012a).

Based on the varying constraint hypothesis on fire activity (Krawchuk and Moritz, 2011), which ranges from fuel limitation in drier areas to drought limitation in wetter areas where fuel is not limiting fire spread, Loepfe et al. (2014) identified these two climatic thresholds as key controls on fire size across Europe. A low quantity and connectivity of vegetation can decrease the burned area despite frequent flammable conditions in dry regions (Pausas and Paula, 2012a). Additionally, recurrent fires can gradually reduce the amount of available fuel, thereby diminishing vegetation combustibility (the speed and intensity with which a material burns) (Ganteaume et al., 2009). Fires in Mediterranean shrub formations (woody species, shrubs, and grasses), which are often highly flammable (Pausas et al., 2017), tend to be more intense and slower than fires in grasslands (grasses) (Dimitrakopoulos, 2002a). The vertical and horizontal continuity of fuels (Keeley et al., 2011a), along with the presence of many small flammable understory vegetation, allows fires to spread to the canopy, thus creating crown fires (Alvarez et al., 2012).

Recent fire activity in Mediterranean Europe is associated with land-use changes and ultimately socioeconomic changes (Chergui et al., 2018). Europe experienced a fire increase in the 1970-1980's to 2000's due to rural depopulation and land abandonment augmenting the occurrence of large fires (Pausas, 2004) and a recent decrease due to increased firefighting expenditures (Ruffault and Mouillot, 2015). Current fire regime in North Africa with small fires is more similar to the European fire regime before the land abandonment period of the 1970's/1980's (Chergui et al., 2018) and has a more stable fire regime over the last decades (Belhadj-Khedher et al., 2018; Kouachi et al., 2024; Madoui, 2002). The western Mediterranean basin is thus marked by a socio-economic gradient between North Africa and Europe, reflected in contrasting forest uses by rural populations firefighting facilities.Fuchs et al. (2013) reconstructed major land-cover classes for 1950–2010 and documented substantial changes at the pixel scale. However, the regional-scale distribution of open vegetation and forests remained relatively stable throughout this period. Although detailed reconstructions are not available for earlier periods in the study area, comparisons with vegetation patterns at 1 ky BP reported by Zanon et al. (2018) indicate that the broad spatial distribution of open vegetation and forests has remained largely unchanged. Together, these findings suggest that land-use changes mainly affect local conditions, while having limited influence on the large-scale vegetation structure considered here.

Our characterisation of recent fire regimes relies on MODIS-derived fire event data from the FRY database (Laurent et al., 2018), which cover only the last two decades and may therefore miss longer-term fire--regime shifts that could be captured by charcoal records. Nevertheless (Loepfe et al., 2014), showed thatfire regimes across Europe and North

Africa during the period 2001-2010 were primarily controlled by climatic humidity thresholds, while vegetation exerted a secondary role through fuel availability. This highlights that large-scale climatic gradients remain the dominant driver of fire–vegetation relationships over decadal timescales, despite local effects of land-use change and socio-economic dynamics.

3. Material and methods

3.1. Marine surface and interface core sediment samples

The sample dataset contains 277 marine surface sediment samples: 102 of which already analysed for microscopic charcoal from the Atlantic margin off the Iberian Peninsula (Genet et al., 2021) and 175 new ones from the western Mediterranean margins (Fig. 1).

The sediment cores were collected during a total of 35 oceanographic cruises (Table S1), conducted between 1981 and 2013, using box, piston and multicore coring method. The samples were obtained from two core repositories in France, EPOC and IFREMER. Depending on the availability of sediments, the samples were taken from the most superficial sections of the sediment cores (Table S1), which allows for analysis of fire changes in recent history.

A potential risk associated with the comparison of the different datasets (charcoal in ocean compared with fire regime, vegetation and climate on land) is that the periods of charcoal records, fire regime characteristics, burnt vegetation type and climate data do not overlap. According to (Müller et al., 1998), core-top of marine sediments cover a few hundred to, at most, a few thousand years corresponding to the late Holocene, which might be problematic when comparing with more recent observations. We synthesized the ages of the marine surface sediment samples using literature data and, when possible, by dating the surface sediment samples using $^{210}Pb_{xs}$ and ^{137}Cs measurements on the bulk sediment by low-back, high efficiency gamma spectrometry (Table S1). Of the 277 surface sediment samples, 2 are modern (high $^{210}Pb_{xs}$ and low ^{137}Cs), 25 are less than 20 years old (moderate $^{210}Pb_{xs}$ and low ^{137}Cs), 20 are less than 60 years old (moderate $^{210}Pb_{xs}$ and higher ^{137}Cs), 14 are between 60 and 100 years old (low $^{210}Pb_{xs}$ and no ^{137}Cs), and 36 more than 100 years old (detectable $^{210}Pb_{xs}$ and no ^{137}Cs) (Table S1). Based on the literature, we estimate that 12 samples are from the late Holocene and 10 are of undetermined Holocene age (Table S1). Dating information available for these 119 samples therefore suggests an age of less than a few centuries. Unfortunately, we were unable to find any dating information in the literature for the remaining 158 samples, and some samples could not be dated because the marine sediment cores had been collected during oceanographic cruises conducted in the 1990s, which is too old for dating using the ^{210}Pb method.

The basis of our comparison of the various datasets is the assumption that the relative differences between hydrographic basins in terms of climate, vegetation, and fire regimes have remained relatively constant over the past century. The methodology employed involved the calculation of the mean of the various environmental data over their respective periods of record to facilitate comparison with microscopic data. It is anticipated that a fingerprint of these spatial patterns will be identified in the microscopic charcoal data. To support the comparison of the different datasets, an investigation was conducted into whether the spatial variability of the microscopic data fell within the range of the variability of microscopic charcoal from the past century. We compared microscopic charcoal concentration values from our marine surface sediment samples with those from 5 short cores located off the Iberian margin (Genet et al., 2021) and 2 short cores collected in the Gulf of Lions (this study) GolHo1B and RHS-KS57 during the GolHo and RHOSOS cruises in 2013 and 2008, respectively (Fig. 1). A multicorer was used to collect the interface core "GolHo1B," while the core "RHS-KS57" was collected with a Küllenberg-type piston corer. For the GolHo1B core (Fig. S1), 14 samples were taken at intervals of 1 cm, covering the period from 1960 to 1998, as dated by $^{210}Pb_{xs}$ (Sicre et al., 2016), giving a mean resolution of 2.7 yr between samples. For the RHS-KS57 core (Fig. S1), 70 samples were taken at intervals of 0.5 cm. The age model was established using 5 chronological points based on a ^{14}C date, the $^{206}Pb/^{207}Pb$ ratio and the vertical distribution of ^{137}Cs (Fanget et al., 2014, 2016). This core covers the period from 1986 to 2005, giving a mean temporal resolution of 0.14 yr between samples.

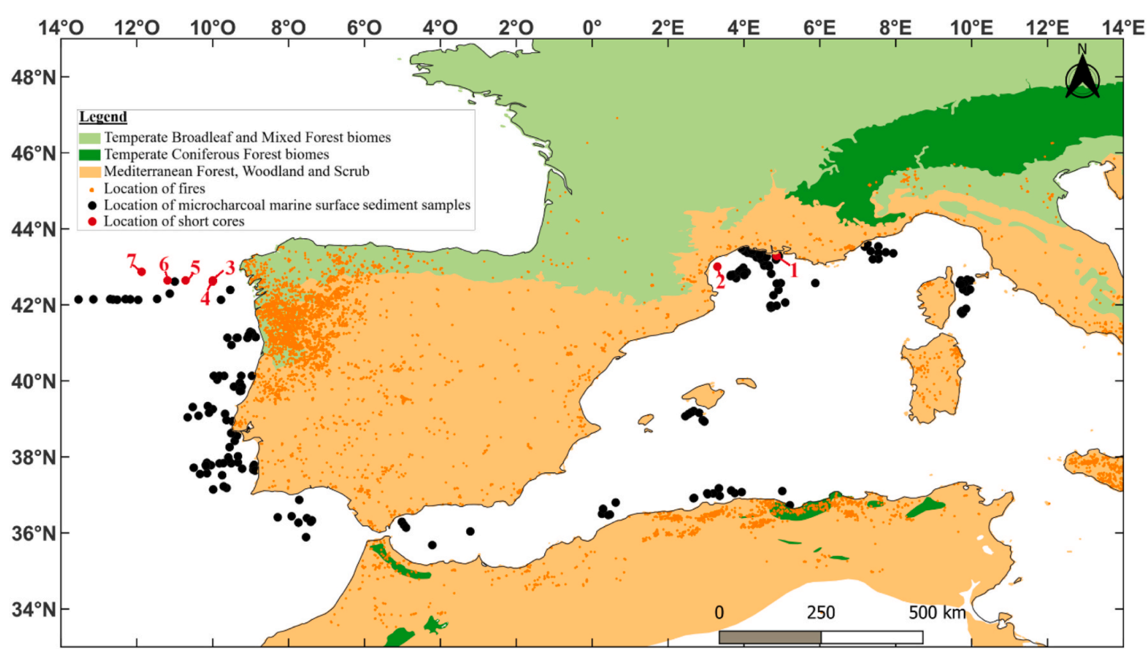

Fig. 1. The study area with its ecoregion: Temperate Broadleaf and Mixed Forest biomes (light green colour), Temperate Coniferous Forest biomes (dark green colour) and Mediterranean Forest, Woodland and Scrub (orange colour) (Olson et al., 2001). Location of fires larger than 25 ha (orange dots) between 2001 and 2016 from the FRY database (Laurent et al., 2018). Location of microscopic charcoal marine surface sediment samples (black dots). Location of short cores (red dots): RHS-KS57 (1), Gol-Ho1B (2), PE109-97-Station4 (3), Pech7I (4), PE109- 97-Station9 (5), PE109-97-Station8 (6), PE109-97- Station6 (7).

3.2. Microscopic charcoal abundance and elongation analyses

The marine surface sediment samples were chemically processed to obtain microscopic charcoal concentrates following Genet et al. (2021), enabling analysis of microscopic charcoal under transmitted and reflected light microscopy (Daniau et al., 2009). About 0.2 g of dry bulk sediment was treated sequentially with 37% hydrochloric acid (HCl) to remove carbonates, 37% nitric acid (HNO_3) 33% hydrogen peroxide (H_2O_2) to eliminate the organic matter, and.

70% hydrofluoric acid (HF) to eliminate siliceous material. The residue was rinsed with HCl to remove colloidal SiO_2 and silicofluorides formed during the HF digestion and then rinsed with distilled water to remove acids. The suspension was diluted (0.1) and filtered through a 0.45 μm membrane (diameter of 47 mm). A portion of the filter was mounted onto a PMMA (Poly Methyl Methacrylate) slide with ethyl acetate and hand-polished using a PRESI polisher (The CUBE) for 4 min with a 400 Angström alumin solution. Subsequently, the slides were scanned with an automated Leica DM6000M microscope at ×500 magnification, with controlled transmitted light adjustment, to detect and measure microscopic charcoal. Only charcoal particles larger than 10 μm were analysed. The maximum particles size considered was 125 μm The detection of microscopic charcoal was based on its black colour using a threshold value in the tint, saturation, and lightness (TSL) colour space. Petrographic criteria in reflected light were used to secure the identification of microscopic charcoal in transmitted light. For each sample, the concentration of microscopic charcoal was calculated as the number of particles per gram dry weight (CCnb in $nb.g^{-1}$) and the total area of all microscopic charcoal in one sample per gram dry weight (CCsurf in $mm^2.g^{-1}$).

The microcharcoal influx (or charcoal accumulation rate), defined as the number of fragments per unit area per unit time, is a common way to study biomass burning in lake sediments (Marlon et al., 2015)., 2016). However, we prefer to use microcharcoal concentration in marine sedimentary sequences because the calculation of microcharcoal influx can be hazardous for different reasons. Firstly, the use of coarse age-depth models can lead to imprecise estimates of sediment accumulation rates. Secondly, an artificially biased microcharcoal influx can occur due to sediment stretching during the coring process or high sedimentation rate events, such as Ice Rafted Debris (IRD) deposits (Daniau et al., 2019). Research undertaken to date has demonstrated a correlation between the distribution pattern of charcoal concentrations and charcoal influx in North Pacific (Mensing et al., 1999) and in eastern Atlantic (Genet et al., 2021) marine sediments. This suggests that charcoal distribution patterns in sediments are not subject to any dilution effect, but instead accurately reflect the sedimentary flux of charcoal particles.

The shape of microscopic charcoal was also analysed using the elongation, i.e. the particles' length to width ratios (L/W) to infer the type of vegetation burned (UmbanhowarJr and Mcgrath, 1998).

3.3. Definition of preferential microscopic charcoal source areas

Aeolian and fluvial processes are the primary transport pathways for charcoal from fire sources to depositional areas (Whitlock and Larsen, 2001). They can be washed out by rain or transported by rivers through processes of rolling and saltation (Nichols et al., 2000). In water, charcoal particles float and sink as they become waterlogged, with the settling rate depending on their size and porosity (Nichols et al., 2000). Small particles can sink within a few hours, while larger ones can float for several months or even years before becoming waterlogged. Microscopic charcoal particles, typically between 10 μm and 100 μm long (Patterson et al., 1987), behave like pollen and other fine terrestrial materials during their journey and eventual deposition in marine environments. Near river plumes, the fine sediments in marine deposits are largely derived from rivers (Heusser, 1983; Naughton et al., 2007). However, in arid areas without water systems, wind becomes the primary means of transporting these small particles (Dupont et al., 2011). The impact of ocean currents on the distribution of pollen in marine sediments is low, and we anticipate a similar effect for microscopic charcoal in our samples (Dupont and Wyputta, 2003). Once in the ocean, these fine particles are incorporated into marine snow and can settle on the seabed within days or weeks (Hooghiemstra et al., 2006).

While microscopic charcoal and pollen exhibit similar behaviour when transported by rivers, they differ slightly when transported by winds due to their unique physical and mechanical properties. Recent models, which take into account elements such as the height at which particles are injected from convective plumes, wind dynamics, the physical properties of the particles and their gravitational deposition, suggest that microscopic charcoal - up to 125 μm - can be deposited within a radius of several to hundreds of kilometres from the fire origin (Vachula and Rehn, 2023). However, the impact of rain or the adsorption of charcoal onto other particles were not considered. To shed light on the origins of microscopic charcoal found in marine sediments, Haliuc et al. (2023) simulated how microscopic charcoal is transported by air and deposited by both dry and wet removal methods. They demonstrated that most microscopic charcoal is deposited within a few hundred kilometres of the fire origin. We anticipate therefore that the majority of charcoal produced within a given hydrographic basin is deposited within the same basin. This microscopic charcoal is then transported to the ocean via the fluvial system.

Although transport processes can lead to fragmentation and abrasion of charcoal particles, experimental studies show that certain morphological parameters, such as elongation, retain a significant structural control and remain partly diagnostic of the original plant material (UmbanhowarJr and Mcgrath, 1998; Crawford and Belcher, 2014; UmbanhowarJr and Mcgrath, 1998). While transport tends to reduce particle size and alter perimeter characteristics, shape metrics such as aspect ratio appear less sensitive to degradation and continue to reflect anatomical properties and fuel type, albeit with increased variability. Morphometric analyses of charcoal particles observed in marine settings offshore the Iberian Peninsula (Genet et al., 2021) and offshore South Africa (Haliuc et al., 2023) show that elongation values (length/width ratio) are generally lower than those obtained in experimental studies (UmbanhowarJr and Mcgrath, 1998; Crawford and Belcher, 2014; UmbanhowarJr and Mcgrath, 1998). However, despite this reduction in absolute values due to transport and fragmentation processes, particle elongation remains consistent with the type of vegetation burned in adjacent drainage basins (Genet et al., 2021; Haliuc et al., 2023), indicating that this morphometric parameter used to infer burned vegetation type is robust. Also, the study of microcharcoal distribution on iberian margin show that the distribution of microcharcoal particles in the ocean floor is independent of their shape, suggesting an homogeneous oceanic transport and deposition (Genet et al., 2021)

In addition, the distribution of pollen in oceanic surface sediments closely mirrors vegetation patterns on nearby land (Dupont and Wyputta, 2003; Genet et al., 2021; Heusser and Balsam, 1977; Hooghiemstra et al., 2006; Morales-Molino et al., 2020; Mudie, 1982). Due to the similar specific gravity of water-saturated microscopic charcoal particles and pollen grains, we assume that microscopic charcoal preserved in marine surface sediments originates from the nearby watershed, thus representing the fire regime at a regional scale (Genet et al., 2021). Consequently, twelve microscopic charcoal deposition zones were defined, along with their respective regional source areas for sedimentary microscopic charcoal, based on the distance from the mouth of the nearest watershed and the marine geomorphology (Fig. 2).

3.4. Climate, fire and burned vegetation data

The global climate database CRU (Climatic Research Unit, CRU CL v. 2.0, grid with a spatial resolution of 10 min, period 1961-1990) from New et al. (2002) was used to obtain monthly temperature and precipitation data for the years 1961-1990. The global fire event database FRY

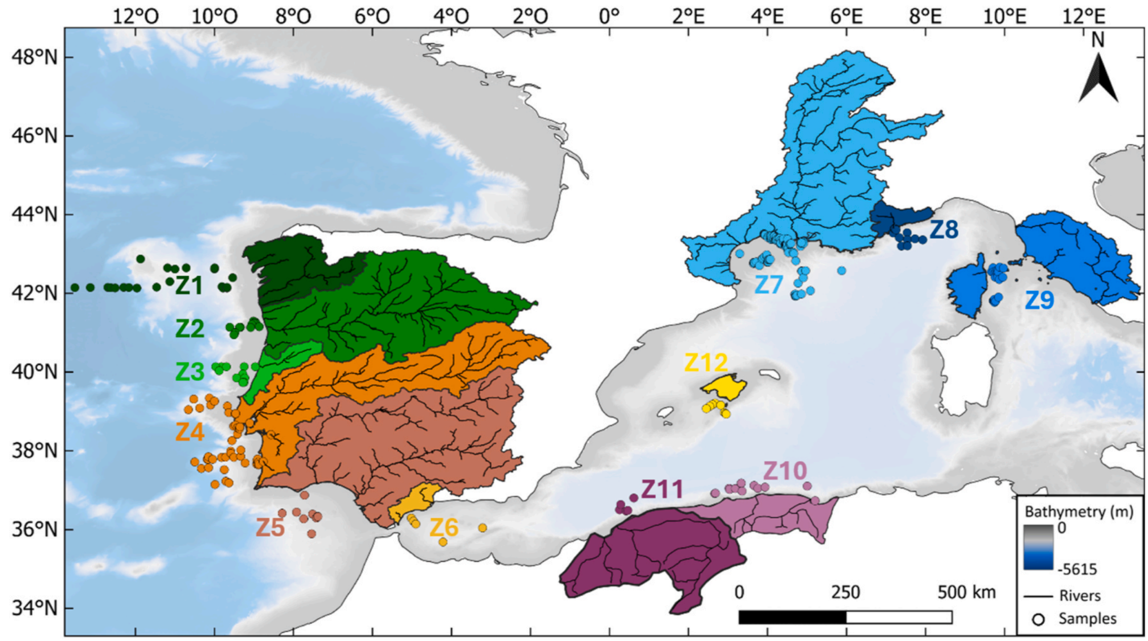

Fig. 2. Marine surface sediment samples (coloured dots) in which microscopic charcoal particles were analysed and their associated land production areas (coloured). The dominant rivers are shown by the black lines.

2001-2016 (Laurent et al., 2018, 2019) using the MODIS MCD64A1 pixel-level 500m resolution (Giglio et al., 2018), with a cutoff value of 12 days for the region (Moreno et al., 2021), and MCD14ML active fire detection for Fire Radiative Power (FRP) as a proxy for fire intensity (Giglio et al., 2016) was used to obtain fire patch characterization (size, shape, intensity, duration and burned vegetation). To ensure consistency in the analysis, we used a uniform grid of 20 × 20 km cells (Fig. S1), enabling the harmonization of comparisons despite differences in database resolution and facilitating the integration of diverse data while maintaining geographical consistency across all terrestrial production zones. Data extraction and map visualization were performed using QGIS software (version 3.22.11; QGIS Development Team, 2022). Thus, the number of fires (FN), the burned area (BA, in ha), and the fire intensity (median Fire Radiative Power) (FRP, in W.m-2) were extracted for each grid pixel. We also calculated the mean fire size in pixels. The FRP index measures the energy emitted by radiative processes released during combustion and can be associated with fire intensity throughout the burning process (Laurent et al., 2018). Climate data (temperature and precipitation) were extracted only from each grid pixel containing fires to provide location-specific climate information. The dominant burned land cover type were extracted from the global fire database FRY (2001-2019) (Laurent et al., 2018). Burned land cover type were then aggregated into 6 sub-classes standardized categories: Cropland, Grassland (Herbaceous vegetation), Mosaic vegetation, Shrublands, Tree-dominated vegetation, Sparse vegetation, and No vegetation (Table S2) based on the Climate Change Initiative (CCI) Land Cover (LC) classification scheme. According to Harper et al. (2023) based on Poulter et al. (2015), mosaic vegetation is composed of grasses (>50%), trees (<25%), and shrubs (25%) and will be considered as open vegetation in this study (Table S2). In this study, 2 burned vegetation classes are defined; tree and shrub vegetation refers to area dominated by woody plants (sub-classes tree, shrub) while open and mosaic vegetation refers to area dominated by non-woody plant (sub-classes Cropland, Grassland and Mosaic vegetation).

3.5. Data analysis

Several statistical analyses were performed and visualized using RStudio Version 1.3.109383 (" RStudio," 2025). The tidyverse package (*tidyverse*, dplyr, tidyr) (Wickham et al., 2019) was used to transform and manipulate the data. Heatmaps were generated using the *pheatmap* package (Kolde, 2025) for visualizations with automatic clustering, and the *ggplot2* package (Wickham et al., 2019) for more flexible representations. Clustering was performed using the *FactoMineR* package (Lê et al., 2008) for the elbow method, and *Factoextra* (Kassambara and Mundt, 2020) to visualize the results. Finally, bar charts and boxplots were created using the *ggplot2* package and specifically geom_boxplot() to compare distributions, medians, quartiles, and outliers between groups.

A k-means clustering analysis was conducted on: (1) the microscopic charcoal data, i.e median values of concentration and elongation for each marine area; (2) the fire parameters, i.e. total number of fires (FN), total burned area (BA), mean fire size (Fs), median radiative power of fires (FRP) in each land zone; (3) climate parameters data, i.e median temperature (T) and median precipitation (P). The Elbow method and the silhouette index were used to determine the optimal number of clusters. The Elbow method identifies this number by finding the point where the decrease in the sum of squared errors (SSE) within clusters forms an elbow, indicating that adding more clusters only marginally improves the SSE. The Silhouette Index, on the other hand, evaluates clustering quality by measuring both the internal coherence of the clusters and their separation from other, with the highest point on the graph indicating the optimal number of clusters. We chose to use both methods because the Elbow method focuses on minimizing clustering errors, while the silhouette index assesses cluster quality. Together, these two analyses help to confirm the choice of the number of clusters to consider.

Boxplots were created to assess the distribution patterns of microscopic charcoal, climate and vegetation data from different areas. Kruskal-Wallis and t-tests were used to explore the differences and similarities in the median and mean values of microscopic charcoal concentration, microscopic charcoal elongation, temperature and precipitation, among the groups obtained from the clustering analysis. A heatmap was created to visualize areas with similar fire regimes (total number of fires (FN), total burned area (BA), mean fire size (Fs), median radiative power of fires (FRP) in each land zone.

4. Results

4.1. Spatial distribution of microscopic charcoal concentration and elongation in marine surface sediments

The CCnb and CCsurf showed a significant and positive correlation (Fig. S3, $r = 0.87$, $p < 0.001$) allowing CCnb to be used to represent regional variability of microscopic charcoal abundance without biases related to fragmentation during production, transport, or laboratory procedures. Of the 277 samples, 12 samples did not contain microscopic charcoal particles, and these samples were removed from the analysis of the elongation ratio.

The CCnb (Fig. 3a) over the whole study area ranged from 0 nb g^{-1} to 1.42×10^6 nb g^{-1}. This range of CCnb in the marine surface sediment samples is within the range of CCnb values recorded by the short cores covering part of the past 130 years (Fig. S4). From this result, we then considered that the mean environmental conditions on land and in the ocean that resulted in the observed CCnb over the past centuries did not significantly deviate from those recorded during the last decades. This finding lends support to our subsequent comparison of microscopic charcoal from marine surface sediment samples with recent observations of climate and vegetation.

When going further in identifying similar microscopic charcoal abundance across watersheds in the study area, the k-means clustering analysis (Fig. 3b) based on the median CCnb values per ocean area (Fig. 3a) (Fig. S5a and b), identified three different groups (Fig. 3b). The first group (Gc1) includes Z1, Z2, Z5 and Z12 (median = 5.27×10^4 nb.g-1, mean = 8.64×10^4 nb.g-1) mostly located off the Iberian Peninsula. The second group (Gc2) includes Z3, Z7, Z8 and Z9 (median = 1.88×10^5nb.g-1, mean = 2.65×10^5 nb.g-1) mostly located off France and Italy, and the third group (Gc3) includes oceanic areas Z4, Z6, Z10 and Z11 (median = 1.97×10^5 nb.g-1, mean = 2.89×10^5 nb.g-1) mostly located off north Africa and Central Iberia (Fig. 3c). The mean CCnb value of Gc1 is significantly different from those of Gc2 (*t*-test: $t = 6.8192$, $df = 190.44$, p-value = 1.179×10^{-10}) and of Gc3 (*t*-test: $t = 6.3308$, $df = 91.511$, p-value = 8.917×10^{-9}). However, the mean CCnb of Gc2 is not significantly different from that of Gc3 (*t*-test: $t = 0.71408$, $df = 126.32$, p-value = 0.4765), so that Iberia (except the watersheds Z3 and Z4) discriminates from other areas.

When analysing further, the mean microscopic charcoal elongation values per ocean area (Fig. 3a–e) ranged from 1.32 to 4.10 (mean = 2,78). The median values per ocean area range from 1.51 to 2.01 (Fig. 3g). A k-means clustering analysis (Fig. 4b) based on the median microscopic charcoal elongation values per ocean area (Fig. S5c and d) reveals 2 different groups (*t*-test = 6.81, df = 190.44, p-value = 1.17×10^{-10}). Mean microscopic charcoal elongation is significantly higher in the western part than in the eastern part (p-value <0.001, Fig. 3g). The first group of elongation (Ge1) includes ocean areas Z7, Z8, Z9, Z10, Z11 and Z12 (mean elongation ratio value of 1.84 ± 0.2), while the second group (Ge2) includes ocean areas Z1, Z2, Z3, Z4, Z5 and Z6 (mean elongation ratio value of 1.97 ± 0.2) (Fig. 3g). The value of 1.8 corresponding to the third quartile value (Q3) for Ge1 (1.84), and to the first quartile (Q1) value for Ge2 (1.83) separates the two groups. Microscopic charcoal elongation values below 1.8 are observed in the eastern part while values above 1.8 are observed in the western part (Fig. 3h).

Although differences among clusters were statistically significant, the low explained variance ($R^2 \approx 0.10$ for concentration and $R^2 \approx 0.06$ for elongation) indicates that cluster membership accounts for only a small proportion of the variability in these metrics. This substantial overlap among clusters suggests that the identified groups represent general structural tendencies rather than well-separated classes. Despite this overlap, the results highlight four contrasted regions, with the Iberian Peninsula experiencing elongated charcoal particles, as opposed to France/Italy and North Africa with squared particles. Within the Iberian cluster, Northern and southern Iberian Peninsula experiencing low charcoal concentrations differentiated from central Iberia experiencing intermediate or high concentration. Within the eastern cluster

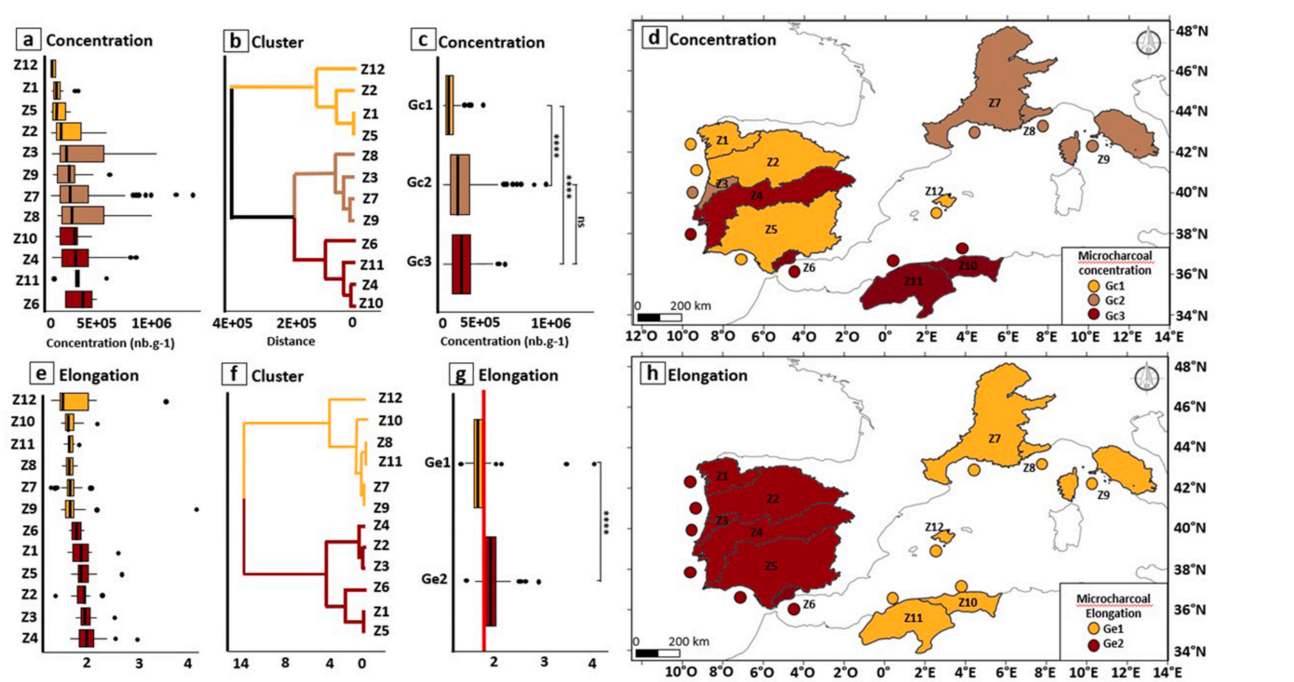

Fig. 3. Microscopic charcoal concentration and elongation values in marine surface sediment samples in each ocean area. (a) Distribution of concentration values across ocean areas. (b) Hierarchical clustering of median concentrations identifying three groups (Gc1 (low), Gc2 (intermediate), Gc3 (high)). (c) Concentration distributions within each cluster. (d) Spatial distribution of median concentrations. (e) Distribution of elongation values across ocean areas. (f) Hierarchical clustering of median elongation identifying two groups (Ge1 (low),Ge2 (high)). (g) Elongation distributions within each group. The red dashed line corresponds to IQ3 value of Ge1 boxplot and, IQ1 value of Ge2 boxplot (value at 1.80). (h) Spatial distribution of median elongation. Colors indicate cluster membership as shown in panels (d) and (h).

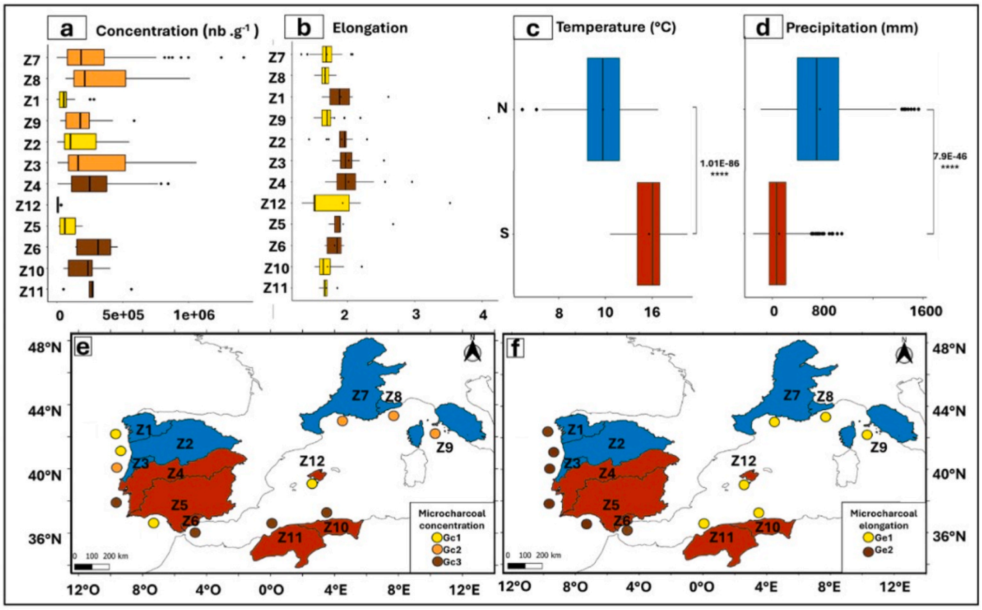

Fig. 4. Relationships between microscopic charcoal characteristics and climate. (a) Boxplot of microscopic charcoal concentration showing the spatial distribution (north–south gradient). (b) Boxplot of microscopic charcoal elongation showing the spatial distribution (north–south gradient). (c) Boxplot illustrating the temperature distribution in the northern region. (d) Boxplot illustrating the precipitation distribution in the southern region. (e) Map of median microscopic charcoal concentration by ocean area and source regions. (f) Map of median microscopic charcoal elongation by ocean area and source regions. Colors indicate concentration (Gc1 (low), Gc2 (intermediate), Gc3 (high)) and elongation (Ge1 (low), Ge2 (high)). Land colors represent climate zones (blue: cool and wet; red: warm and dry).

with squared particles, North Africa experiencing high concentration, differentiated from France and Italy experiencing intermediate concentration.

4.2. Comparison between microscopic charcoals and climate

The northern (north of 40°N) and southern parts (south of 40°N) of the study area have significantly different climates (Fig. 4c and d; Fig. S6) (temperature: p-value $<1.01\ \text{x}10^{-86}$; precipitation: p-value $<7.9\ \text{x}10^{-46}$). The northern part has a cool and wet climate, with a mean annual temperature of 11.8 ± 0.1 °C (Fig. 4c) and a mean annual precipitation of 779.1 ± 17.89 mm (Fig. 4d). The southern part has a warmer and drier climate, with mean annual temperature of 15.8 ± 0.1 °C (Fig. 4c) and a mean annual precipitation of 455 ± 7.1 mm (Fig. 4d).

Across this climate gradient, the trend shows that microscopic charcoal concentrations are higher in the southern region (below 40°N) (Z4, Z6, Z10, Z11) than in the northern region, except for Z5 and Z12 (Fig. 4a–e). Higher microscopic charcoal concentrations appear to be associated with warmer and drier climates. In contrast, lower microscopic charcoal concentrations (Z1, Z2, Z3, Z7, Z8 and Z9) are observed in regions with cooler and wetter climates (Fig. 4). Elongated or squared particles are present regardless of the climates. A low elongation of microscopic charcoal (Ge1) (yellow dots in Fig. 4b–f) is associated with a cool and wet climate in Z7, Z8 and Z9 and with a warm and dry climate in Z10, Z11 and Z12. A high elongation of microscopic charcoal (Ge2) (brown dots in Fig. 4b–f) is associated with a cool and wet climate in Z1, Z2 and Z3 and with a warm and dry climate in Z4, Z5 and Z6. This result highlights the non-straightforward relationship between microscopic charcoal elongation and climate across the region, thus requiring a deeper understanding of additional charcoal particles drivers.

4.3. Assessment of microscopic charcoals relationship with fire regimes (frequency, burned area, fire radiative power, fire size)

In order to assess how marine charcoal information could be related to inland complex fire regimes not fully related to the climate gradient, we analysed fire regime characteristics (total burned area, fire number, size, intensity) which revealed significant differences across areas. Considering the results of the elbow method and silhouette score analysis, we chose to consider 2 and 4 groups. This approach allows us to combine an overview (2 groups) with a more detailed exploration (4 groups), further ensuring a rich and coherent interpretation consistent with the charcoal analysis (Section 3.1), climatic observations (Section 3.3) and burned vegetation (Section 3.4). Two groups of fire regimes can be distinguished based on the number of fires and burned areas. The first group (GA) characterized by frequent fires and a high total burned area (Fig. 5a, red dendrogram), is mostly located in Iberia and North Africa (zones Z2, Z4, Z1, Z10, Z5 and Z11). The second group (GB) characterized by rare fires and a low total burned area (Fig. 5a, blue dendrogram) is mostly located in France and Italy (zones Z8, Z6, Z7, Z9, Z3 and Z12). However, the parameters related to average fire size and intensity vary greatly within these two groups and necessitate finer-scale analysis into four subgroups (GA1, GA2, GB1, GB2). Within GA, characterized by frequent fires and a high total burned area, GA1 (light pink) observed in zones Z2 and Z4 stands out for its large and intense fires (orange). GA2 (dark pink), on the other hand, is observed in zones Z5, Z11, Z1 and Z10 and stands out for its low intensity fires (yellow), associated with small (Z1, Z10) or large (Z5, Z11) fire sizes. For group GB, characterized by rare fires and a low total burned area, GB1 (light green) mostly observed in France (Z6 and Z7) stands out for its small and intense fires except for Z8 (low fire intensity). GB2 (dark green) is mostly observed in Italy, Corsica and Balearic Islands (zones Z3, Z9 and Z12) and stands out for its large and intense fires.

Our fire data analysis confirms that the fire regime in the western Mediterranean basin follows a north-south climatic gradient with rare, small and more intense fires in the northeastern regions (GB: France, Italy), compared to more frequent, larger and less intense fires in the south (GA: Algeria, Spain, and Portugal). However, northern Iberia (Z1 and Z2) experiences more frequent and larger fires (GA) yet characterised by cool and wet climate (Fig. 4). Z6 and 12, although being in the warm and dry climate region, present rare and small fires (GB).

Low (Gc1, yellow dots in Fig. 4b) and intermediate (Gc2 orange dots in Fig. 4b) charcoal concentrations are observed on the island of Majorca

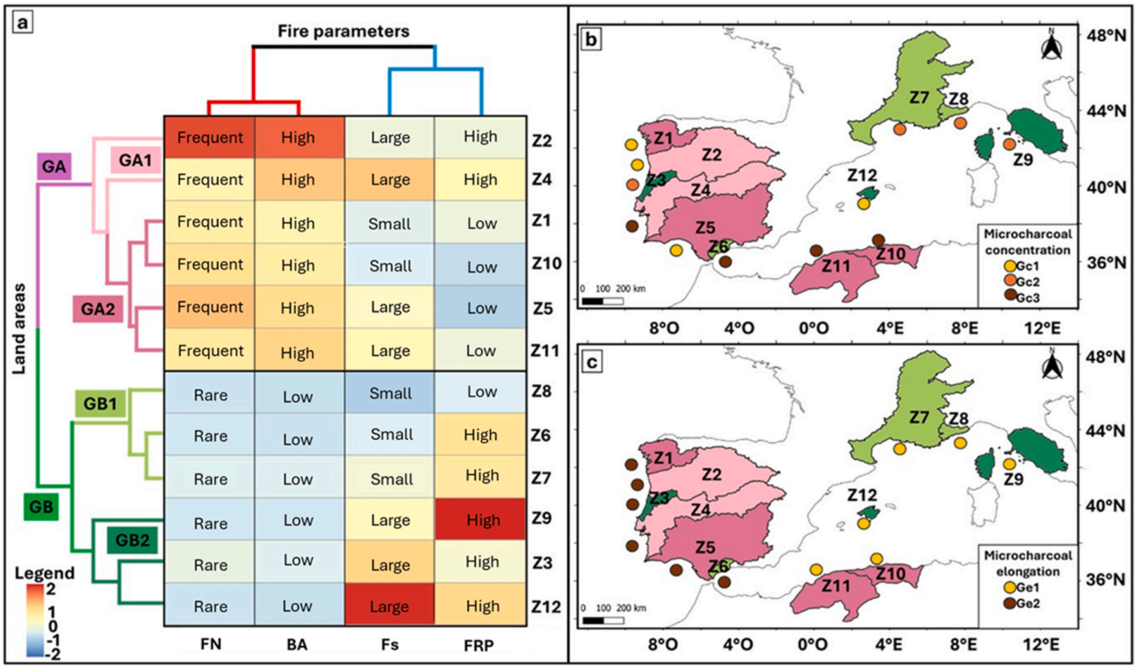

Fig. 5. Relationships between fire regime parameters and microscopic charcoal characteristics.(a) Heatmap and clustering of fire regime parameters across land areas (FN: number of fires, frequent >530 fires; BA: burned area, high $>10 \times 10^4$ ha; Fs: fire size, high >700 ha; FRP: fire radiative power, high >75 Watt). Dendrogram shows similarities between land areas. Two main clusters (k-means, validated by elbow and silhouette methods) are indicated in blue and red, and four subgroups (GA1, GA2, GB1, GB2) are shown by surrounding colors. The color scale indicates increasing values from low (blue) to high (red).(b–c) Maps of median microscopic charcoal concentration and elongation, respectively. Colors indicate concentration (Gc1 (low), Gc2 (intermediate), Gc3 (high)) and elongation (Ge1 (low), Ge2 (high)). Land areas are coloured according to fire regime groups (GA1, GA2, GB1 and GB2).

(Z12), in France and Italy (Z7, Z8 and Z9), and in central Iberia (Z3), associated with a GB-type fire regime (rare fires with a low burned area). These patterns likely reflect conditions of limited fire activity and/or reduced biomass availability, leading to lower charcoal production. Higher charcoal concentrations (Gc3, brown dots in Fig. 4b) are recorded in North Africa (Z10 and Z11) and in the Tagus Basin (Z4), associated with a GA fire regime (frequent fires and a high total burned area). This association is consistent with high fire activity, leading to increased charcoal production. Low charcoal concentrations (Gc1, yellow dots in Fig. 4b) are also observed in the north and southwest of the Iberian Peninsula (Z1, Z2 and Z5), despite being associated with a GA-type fire regime (frequent fires and a high total burned area). This discrepancy suggests that charcoal concentration is not solely controlled by fire activity, but is also influenced by additional factors such as vegetation type, fuel characteristics, or climatic conditions. High charcoal concentrations (Gc3, brown dots in Fig. 4b) are also observed in the south of the Iberian Peninsula (Z6), associated with a GB fire regime (rare fires and a low total burned area) which suggests that vegetation type, or climatic conditions leading to changes in fuel moisture status, could alter charcoal abundance.

When looking at the correspondence between fire regimes and charcoal concentration, we could not find any relationship between charcoal concentrations and fire regimes (GA and GB). Higher charcoal concentrations values (Gc3) found in North Africa (Z10 and Z11) and Tajo basin (Z4) actually correspond to more burned area and fire number (GA fire regime), yet low charcoal concentrations values (Gc1) observed in Z1, Z2 and Z5 correspond to the same fire regime, thus limiting the interpretation of charcoal concentrations as a surrogate for burned area or fire frequency.

The GB fire regime with rare events and lower burned area mostly correlates with intermediate Gc2 charcoal concentration, although other charcoal concentrations groups were observed for small watersheds as Z12, Z6 and Z3. This indicated that charcoal concentration alone cannot be interpreted as a direct proxy for burned area or fire frequency.

Squared microcharcoal particles (Ge1, yellow dots in Fig. 4c) and elongated particles (Ge2, brown dots in Fig. 4c) are also associated with both fire groups GA (pink in Fig. 4a) and GB (green in Fig. 4a). For example, GA is actually associated to either high concentration of squared charcoal particles (Z10, Z11 in North Africa), or low concentrations of elongated particules (Z1, Z2, Z5 in Iberia). This variability suggests that particle morphology reflects additional controls beyond fire regime alone, such as fuel type or transport processes. However, within similar particle shape conditions, a pattern emerged when considering charcoal elongation in addition to concentrations: GA and GB fire regimes are well discriminated among similar squared particles charcoal signal, so that north Africa (Z10 and Z11) experiencing higher concentrations belong to high burned area and frequent fires, while France and Italy (Z7 Z8 and Z9) experiencing lower concentrations belong to rare fires and low burned area. These results suggest that concentrations partially capture fire regimes and is a function of other variables. In addition, particle elongation should be considered for robust conclusions on fire regimes identification based on charcoal particle concentration data.

4.4. Assessment of burned vegetation impact on microscopic charcoal

Based on the previous section capturing the link between charcoal concentration and burned area, but only when additionally considering charcoal elongation, we tested whether this elongation information was related to vegetation burned. Over the recent period when remote sensing information is available, the western and eastern parts of our region are characterized by different types of burned vegetation (Fig. 6f and g). In the western part (Z1, Z2, Z3, Z4, Z5 and Z6), the percentage of burned tree and shrub vegetation remains below 35% (below the red line, Fig. 6c). In contrast, in the eastern part (Z7, Z8,Z9, Z10 and Z11), this percentage exceeds 35% (above the red line, Fig. 6c).

No relationship is observed between charcoal abundance and burned tree and shrub vegetation. Low microscopic charcoal concentrations

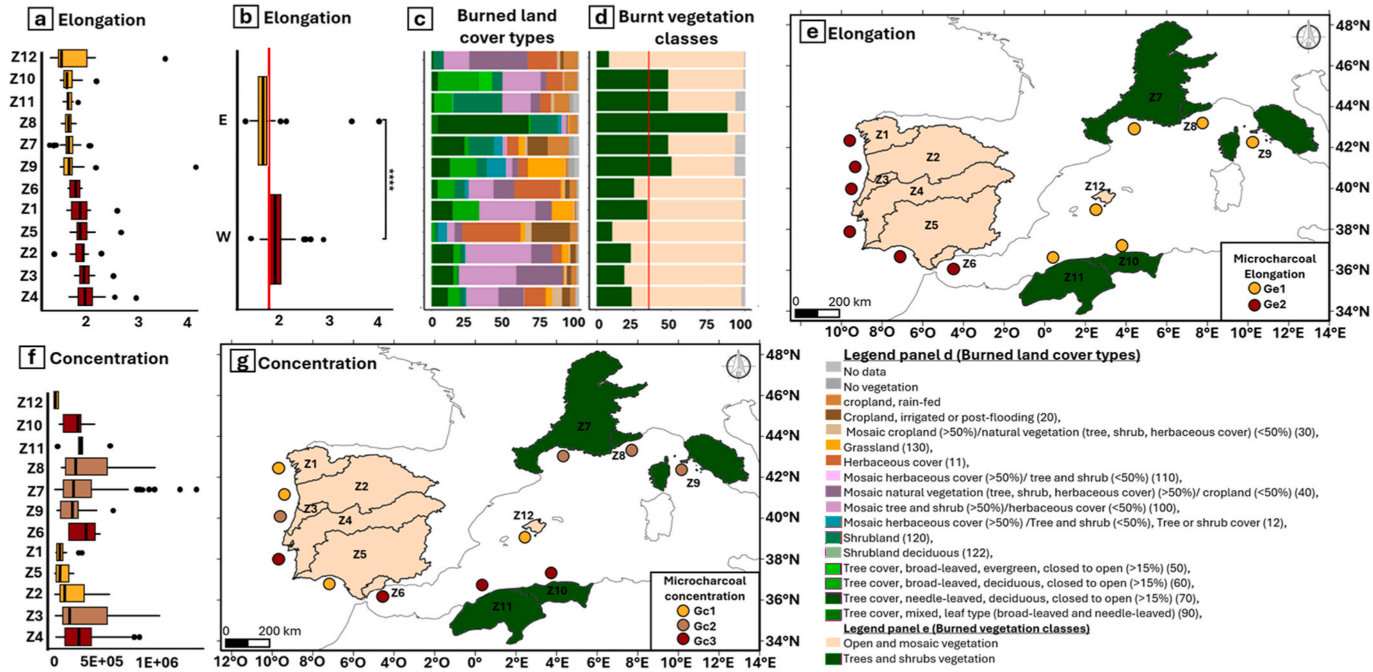

Fig. 6. Comparison between microscopic charcoal concentration and elongation, and burned vegetation types. a: Boxplots of microscopic charcoal elongation measured in marine sediment samples for each ocean area arranged in ascending order from the top to the bottom. a, b, c, d are classified in the order of increasing elongation from top to bottom.b: Boxplots of microscopic charcoal elongation in the eastern and western regions. Red dashed line corresponds to value at 1.80. c: Bar plot of burned land cover types in each land area d: Bar plot of burned vegetation classes representing percentages of burned tree and shrub (dark green) and of burned open and mosaic vegetation (beige) and no and sparse vegetation (grey) in each land areas. The red line in (d) represents a distinction between the percentage of burned vegetation of trees and shrubs and open vegetation at the value of 35%. e: Map representing the median microscopic charcoal elongation for each ocean areas (dots) associated with their source areas on land. e: f: Boxplot of microscopic charcoal concentration for each ocean area with low (Gc1) (yellow), intermediate (Gc1) (orange) and high (Gc3) (brown) concentration. g:Map representing the median microscopic charcoal concentration for each ocean areas (dots) associated with their source areas on land. Colors in land in maps (e and g) correspond to land where the burning of tree and shrub vegetation exceeds 35% (green) or does not.

(Gc1) (yellow dots in Fig. 6a–f) are observed only in areas where burned tree and shrub vegetation exceeds 35% i.e, burned open and mosaic vegetation exceeds 75% (Z1, Z2, Z5, and Z12). Intermediate concentrations (Gc2) (orange dots in Fig. 6a–f) occur both in areas with burned tree and shrub vegetation exceeds 35% (Z7, Z8, and Z9) or falls below 35% (Z3). Likewise, high concentrations (Gc3) (brown dots in Fig. 6a–f) are found in areas where burned tree and shrub vegetation exceeds 35% (Z10, Z11) as well as where it is below 35% (Z4, Z6). Elongated microscopic charcoal particles (Ge2) (brown in Fig. 6d,e,g) are found in areas where the percentage of burned tree and shrub vegetation (Fig. 6c) does not exceed 35%, (Z1-Z6) while squared microscopic charcoal particles (Ge1) (yellow in Fig. 6d, e, g) are present in areas where this percentage exceeds 35%, (Z7-Z11) except for Z12 (<35%). This major result thus confirms that charcoal particles elongation captures vegetation burned. When combined with charcoal concentrations, paleorecords can then capture gradients of fire regimes within vegetation types, that can be inferred from elongation as a keystone information for robust interpretation.

5. Discussion

5.1. Morphology of microscopic charcoal captures tree vs grass burning

Experimental combustion studies have shown that charcoal particle elongation is strongly related to fuel type. Measurements performed from isolated particles produced under controlled combustion of different plant types, allows the establishment of distinctive thresholds between fuel types. Results show that wood-derived charcoal generally exhibits ratios <2, whereas herbaceous-derived charcoal is more elongated, with values > 3 and in some cases reaching up to 11.5 (Table 1) (Crawford and Belcher, 2014; Feurdean, 2021; Inoue and Usuki, n.d.; Pereboom et al., 2020; UmbanhowarJr and Mcgrath, 1998). According to Feurdean (2021), squared charcoal particles are produced during crown fires that consume trees, while elongated particles result from surface fires mainly affecting grasses.

In marine settings, Haliuc et al. (2023) report lower values, with a ratio >2.1 ± 0.5 corresponding to savanna or open grassland fires in subtropical Africa, whereas a ratio <1.8 ± 0.3 reflects forest fires in equatorial and tropical regions (Table 1). These differences may be due to the diversity of charcoals present in marine samples, their degradation during transport, or laboratory processing, all of which can reduce the elongation ratio of microcharcoal (Crawford and Belcher, 2014; Inoue and Usuki, n.d.; UmbanhowarJr and Mcgrath, 1998). Furthermore, transport, fragmentation, and post-depositional processes may reduce charcoal elongation values in marine environments. As a result, thresholds established from experimental combustion studies cannot be directly transferred to sedimentary archives and must be calibrated within each depositional context. However, as previously observed by Genet et al. (2021), the individual elongation values of our most elongated microcharcoal particles are very similar to those produced in laboratory experiments (Fig. S2).

Nevertheless, several studies indicate that elongation remains a robust indicator of burned vegetation type. Although transport processes can lead to fragmentation and abrasion of charcoal particles, experimental studies show that certain morphological parameters, such as elongation, retain a significant structural control and remain partly diagnostic of the original plant material (UmbanhowarJr and Mcgrath, 1998; Crawford and Belcher, 2014; UmbanhowarJr and Mcgrath, 1998). Consistent with this interpretation, morphometric analyses of marine charcoal offshore the Iberian Peninsula (Genet et al., 2021) and South Africa (Haliuc et al., 2023) demonstrate that elongation values continue to reflect the dominant vegetation of adjacent drainage basins

Table 1
Summary of studies measuring charcoal aspect ratios from experimental burning (white row), in marine sediments (light grey row) and in lacustrine sediments (dark grey row).

Reference	Ecosystem / Geographic Context	Combustion Type	Elongation Value	Fuel Type Interpretation
Crawford & Belcher (2014)	United Kingdom (temperate)	Ovens	~1.97	Wood
			3.7	Herbaceous
Umbanhowar Jr. & McGrath (1998)	North America	Open combustion	2.23 ± 0.1	Wood
		Muffle furnace	2.13 ± 0.13	
		Open gcombustion	4.83 ± 0.27	Herbaceous
		Muffle furnace	3.62 ± 0.15	
Feurdean et al., 2021	Siberian Taiga	Muffle oven	6.7 to 11.5	Herbaceous
			2.1 to 3.5	Leaves
			2 to 5.2	Wood and twigs
Feurdean et al., 2023	Temperate herbaceous ecosystems	Muffle oven	> 3	Herbaceous
Inoue & Usuki (2025)	Japan	Open combustion	> 3	Herbaceous
Vachula et al.,2021	Various		< 2.5	Wood
			> 3.5	Herbaceous
Haliuc et al., 2023	Subtropical Africa and tropical regions		> 2.1 ± 0.5	Herbaceous
			< 1.8 ± 0.3	Wood
Aleman et al. 2013	Tropical grassy ecosystems		> 2 (W/L<0.5)	Graminoids
Leys et al., 2015	Grass prairie ecosystems of North America		> 2 (W/L<0.5)	Graminoids

despite lower mean elongation values than those observed experimentally. Furthermore, Genet et al. (2021) showed that the distribution of microcharcoal particles on the Iberian margin is independent of particle shape, suggesting that oceanic transport and deposition do not selectively sort charcoal according to elongation. Together, these results support the use of charcoal elongation as a reliable proxy for inferring burned vegetation types in marine sediment records.

The mean elongation ratio observed in our study is below 1.8 in the eastern part and above 1.8 in the western part, values lower than those reported in laboratory experiments but consistent with observations in marine environments (Genet et al., 2021; Haliuc et al., 2023). In the eastern part (Z7–Z12, Mediterranean climate), a mean elongation ratio <1.8 is associated with the burning of woody vegetation (>35% trees and shrubs). This mean elongation ratio of <1.8 ± 0.1 closely matches the values reported by Haliuc et al., (2023) (<1.8 ± 0.3) in marine surface samples reflecting forest fires off equatorial and tropical Africa. We suggest that fuel continuity, sufficient moisture, and flammable Mediterranean understory allow fires to reach the canopy (Alvarez et al., 2012; Keeley et al., 2011b), resulting in the combustion of wood and leaves, which explains the presence of squared-shape particles off forested-ecosystems (Feurdean, 2021).

In the western part (Z1–Z6, temperate and Mediterranean climates), a ratio above 1.8 reflects the burning of relatively open vegetation (<35%) and suggests, according to (Feurdean, 2021), surface fires producing elongated particles. However, this value differs from the higher values (>2.1 ± 0.5) reported by Haliuc et al., (2023) for open grassland-savanna fires. Similar thresholds (>2) have, however, been identified in lacustrine sedimentary archives for tropical savanna ecosystems (Aleman et al., 2013) and North American grasslands (Leys et al., 2015). These results suggest that herbaceous-dominated ecosystems can increase the mean elongation ratio in sedimentary archives.

Zone Z12 is an exception to this pattern. We assume that the squareshaped microcharcoal particles observed at this site originate from fires in a “mosaic natural vegetation” (Fig. 6b), where the burned area includes >35% trees and shrubs. This type of vegetation comprises more than 50% tree, shrub, and herbaceous cover and less than 50% cultivated land (Table S2).

Although neither our study nor that of Haliuc et al. (2023) covers all vegetated ecosystems, both confirm that relative variations in elongation ratios in marine sediments provide a useful proxy for distinguishing microcharcoal sources from crown fires in forests (lower values) versus surface fires in herbaceous formations (higher values). In addition, they suggest that a mean elongation ratio around 1.8 provides a useful empirical reference for distinguishing charcoal assemblages dominated by woody fuels from those associated with more open, herbaceous vegetation in marine sediment records. However, this value should be regarded as context-dependent and may vary according to ecosystem characteristics, transport pathways, and analytical procedures, rather than a universal threshold.

5.2. Combined information on the morphology and abundance of microscopic charcoal capture fire regimes and climate

We showed that fire regimes in the western Mediterranean basin are influenced by the climate, which changes from north to south (Pausas et al., 2017; Pausas et Paula, 2012). The abundance of charcoal can be driven by different characteristics of fire regimes or fuel characteristics, which in turn are governed by climate and vegetation (Marlon et al., 2006). In Europe, recent studies of lacustrine sediments have shown that the presence of charcoal can be a reliable indicator of the areas affected by fire, as well as the recurrence of such events (Adolf et al., 2018). Modern marine sediments off Iberia indicate a correlation between charcoal abundance and the size and intensity of fires (Genet et al., 2021). The abundance of charcoal in marine sediments reflects the extent of burned areas in California (Mensing et al., 1999), another region under a Mediterranean climate. Research indicates a correlation between charcoal abundance and specific elements of the fire regime. However, it is evident that fuel and climate have a significant impact on charcoal abundance. A higher abundance of charcoal has been recorded in Mediterranean biomes than in temperate and boreal biomes, in relation to a dry-wet climatic gradient (Adolf et al., 2018). The same pattern was identified in marine sediments off Iberia, with reduced accumulation off northern Iberia attributed to small, low-intensity fires burning wooded vegetation in a cool and wet climate, as opposed to the larger and more intense fires burning open Mediterranean woodland under a warm and dry climate observed off southern Iberia (Genet et al., 2021).

Our results on charcoal concentration suggest that direct relationships with fire regime parameters, burnt vegetation types and climate conditions are difficult to establish, highlighting the complex and multifactorial nature of charcoal production, transport and deposition. At the basin scale, no clear relationship could be established between charcoal concentration and climate, with only broad-scale patterns emerging at the subcontinental scale. Even when using a more detailed climatic subdivision (as shown in the box-plot analysis in Fig. S7), refining the climatic framework does not provide additional explanatory power for concentration patterns. In contrast, a clearer signal emerges when considering fire regimes: rare and small fires are associated with cool and wet conditions, whereas warm and dry conditions correspond to more frequent and larger fires, as well as higher charcoal concentrations. This indicates that climate–vegetation–fire relationships are internally consistent within a given vegetation type. To synthesize the main patterns identified in our dataset, we propose the conceptual framework shown in Fig. 7. This framework is not intended to represent a single causal pathway but rather to summarize the dominant relationships observed between charcoal abundance, fire regime characteristics, main burned vegetation types, and climate.

Within ecosystems sharing similar burnt vegetation types (open vegetation versus forest), as identified by the elongation ratio, increasing charcoal abundance is generally associated with a change in fire regimes, from rare fire and low burned areas (open vegetation, Z3, Z12; forest, Z7, Z8 and Z9) to frequent and large burned areas (open vegetation, Z4; forest, Z10 and Z11) (Fig. 7). Z12 (Majorca Island), in particular, experiences extremely rare fires (only 5 recorded) and a low burned area, which likely restricts microscopic charcoal production. These correspondences reinforce the idea that fire frequency and the extent of burned areas are important determinants of charcoal inputs (Adolf et al., 2018; Mensing et al., 1999). These patterns demonstrate

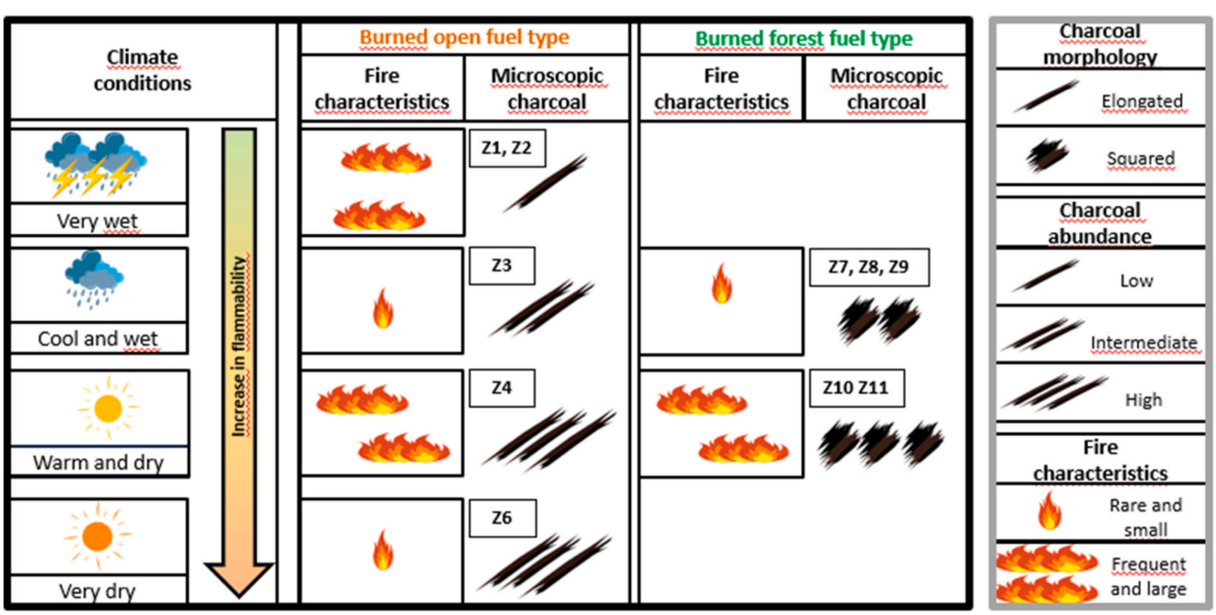

Fig. 7. Schematic representation of how climate and type of burned fuel impact the abundance and morphology of microscopic charcoal observed in marine surface sediments. Variation in the microscopic charcoal concentration (1 particle = low concentration, 2 particles = intermediate concentration, 3 particles = high concentration) and in microscopic charcoal morphology (elongated or squared) depending on the latitudinal climatic gradient (left panel), the type of main burned fuel with fire frequency and burned area (open in central panel and closed in right panel).

also a close correlation with climate, as the variations in charcoal abundance also follow the climatic gradient from cool and wet to warm and dry climates, suggesting climate as another major control of fire regimes captured in charcoal abundance (Adolf et al., 2018; Genet et al., 2021) (Fig. 7). In such conditions, humidity limits flammability, while drought enhances flammability (Pausas et al., 2017; Pausas and Paula, 2012b). The resulting pattern is consistent with the fire–fuel–climate relationship (Pausas and Paula, 2012b), suggesting that charcoal production arises from the coupled interactions among fuel availability, fire activity, and flammability, rather than being controlled by any single dominant factor.

5.3. Limitations and uncertainties

Despite a substantial and meaningful interpretation of the charcoal signal in relation to current fire regimes and their drivers, we acknowledge our analysis also reveals discrepancies that nuance this relationship. Our approach inherently, faces a temporal mismatch between the two main sources of information. On the one hand, microscopic charcoal data from marine sediments provides an averaged signal of fire regime variability over periods spanning a few decades to a few centuries. On the other hand, the environmental data used to characterize climatic conditions, burned vegetation, and fire regimes are derived from satellite observations, which capture only the most recent phase of fire-regime behaviour, and incorporate a significant human influence on fire regimes. We recognize that this mismatch, combined with the dynamic nature of land-use change and anthropogenic influences, limits the extent to which spatial patterns can be assumed to be stable over the past century. Although both datasets are aggregated at the catchment scale, they reflect different aspects of the fire–vegetation system and therefore provide complementary rather than directly equivalent information. The integration of catchment-scale fire signals is nonetheless consistent with the emergence of larger-scale fire regime structures, such as the pyroregions described by Galizia et al. (2022).

Fire regimes are strongly constrained by climatic humidity thresholds, with vegetation influencing fire activity through fuel availability (Loepfe et al., 2014). In this context, sedimentary charcoal records provide a proxy for regional fire regimes, whereas MODIS-derived vegetation structure captures present-day vegetation patterns that are broadly organised along bioclimatic gradients, although locally modified by land use and human activities. Overall, the integration of catchment-scale fire signals is consistent with the emergence of larger-scale fire regime structures, such as the pyroregions described by Galizia et al. (2022).

Recent fire reconstruction since the 1980's from Landsat images over the region (Díaz-Delgado et al., 2004; Kouachi et al., 2024) could provide additional insights into the temporal dynamic of fire regimes, yet not fully and homogeneously covering the whole region. Long-term archival fire records for Algeria, spanning more than 160 years (1860 to the present), constitute a key source of evidence on past fire regimes prior to the advent of Earth-observation satellites (EOS) (Madoui, 2002; Meddour-Sahar et al., 2008).

It was not anticipated that the charcoal concentration in Z1 and Z2 (Northen Iberia) would be so low, given the prevalence of frequent fires and large burned areas in northern Iberia. Northern Iberia experiences frequent and large fires (GA) yet characterised by a cool and wet climate (Fig. 4). The high summer thunderstorm activity in this region (Pugnet et al., 2010) is likely responsible for this discrepancy. In addition, Eucalyptus forests dominate the region, an introduced species in the late 19th century for private owners, with a high propensity to generate and tolerate fire. This forest grew from 115,000 ha in the 1960's to 389,000 ha in the 1990's (Ruiz and Lopez, 2010), so that forest cover and burned area derived from the 2002-2019 fire observations might overestimate forest contribution compared to charcoal data.

The elevated charcoal concentration in Z6 and Z12 was not anticipated neither, given the low fire frequency and reduced burned areas that could be caused by low vegetation amount and connectivity (Pausas and Paula, 2012b). An enhanced flammability driven by warmer and drier conditions in this region could explain this pattern. In addition, this area is dominated by graminoids-mixed vegetation fires (Fig. 6) that might contribute to a high abundance of charcoal in marine sediments (Genet et al., 2021; Haliuc et al., 2023) (Fig. 7). Low concentrations are observed also in Z5 under a warm and dry climate while experiencing frequent fires and large burned areas. Genet et al. (2021) suggested that the burning of "cropland" can produce small amounts of elongated microscopic charcoal. Furthermore, the low intensity of fires, facilitated by the presence of fine biomass and rapid moisture loss (Dimitrakopoulos, 2002b), may lead to partial combustion, thus limiting charcoal production in a region where over 80% of the burned vegetation is open, including more than 25% cropland.

Also, we cover here countries with constrasting socio-economic contexts and firefighting facilities, particularly when including Algeria, outside of the EU. The latter has considerably increased investment in fire-prevention infrastructure, notably in aerial firefighting resources and monitoring systems alongside an updated national forest policy, following the deadly 2021 and 2022 fires, which caused 157 fatalities and unprecedented ecological and socio-economic damage (Bank, 2023; Kouachi et al., 2024). We interpreted the North-South gradient of charcoal concentration as a robust indicator of the burned area gradient observed across France, Italy and Algeria, and as a response to increasing drought and temperature when going southward (Fig. 7). Algeria with 2.95% of burnable land affected yearly by fires (Kouachi et al., 2024), is indeed the most affected country when compared to France (0.53%) and Italy (1.4%) as reviewed in Majdalani et al. (2022). However, neighbouring Tunisia with a similar Saharan influence as Algeria (Belhadj-Khedher et al., 2020), experiences only 0.19% of its burnable land affected by fire, due to high fire prevention and forest safety (Belhadj-Khedher et al., 2020). Despite important contextual similarities, forest fire causes across Europe (Ganteaume et al., 2013) and Algeria (Meddour-Sahar et al., 2013a) differ. Based on a 20-year fire causality analysis (2000-2020), only 25% of causes in Algeria are identified with naturally ignited fires being practically absent (Bank, 2023; Meddour-Sahar et al., 2013a). The predominance of unknown causes masks a large share of intentional and even security-related fires (Meddour-Sahar et al., 2013a; Meddour-Sahar et al., 2013b). Conversely, in Mediterranean Europe (2006-2010), 71% of fire events had an identified cause, with around 5% attributed to natural origins (Ganteaume et al., 2013). Furthermore, distinct fire policies and rural population challenges (Meddour-Sahar, 2015) coupled with periods of political instability and adverse security conditions (Arfa et al., 2009; Meddour-Sahar et al., 2013a), further widen these differences. In turn, although the relationship between charcoal particles and fire regime from remote sensing is meaningful, its link to climate might be enhanced by this socio-economic gradient. That should be carefully considered when covering countries with contrasting Gross Domestic Product (GDP) and Human Development Index (HDI) (Forrest et al., 2024), or road density network (Bowring et al., 2024) as key drivers used in global fire models.

Fire regimes can vary within watersheds that have been identified as sources of charcoal particles from marine cores. For example, the extended Rhone river basin in France covers both the Mediterranean fire-prone region and the low burning Alpine region (Barbero et al., 2019), and the Algerian watersheds cover the humid to arid ecosystems with contrasted fire drivers (Curt et al., 2020), potentially rendering marine charcoal interpretation more complex. However, the approach that was adopted examined the relationships between charcoal, fire regimes, climate, and burnt vegetation types, by using information extracted from each grid pixel containing fires in order to limit this bias.

5.4. Implications for the interpretation of paleofire records

Our study highlighted several indicators that could facilitate the interpretation of marine paleofire records (Genet et al., 2025), with caution for charcoal abundance. We propose a two-step approach for paleo-fire studies, combining particle morphometry analysis with charcoal quantification. Firstly, the reconstruction of the type of burned vegetation can be inferred from the elongation of charcoal particles. As stated in the research by (Feurdean, 2021), this information could also help identifying the occurrence of crown fires (square particles) versus surface fires (elongated particles). Secondly, pollen studies (e.g., Fourcade et al., 2024; Joannin et al., 2012; Lambert et al., 2020; Marquer et al., 2014) should be used to infer potential changes in the stability of vegetation and fuel types. This information is crucial for assessing whether changes in charcoal abundance are influenced by changes in vegetation type or a change in the fire regime. We demonstrated that the abundance of charcoal in marine sediments located off forested ecosystems is primarily driven by fuel type and flammability. The abundance is lower in samples off the Atlantic forests than off the closed Mediterranean forests (where more than 35% of trees and shrubs have been burnt). When considering only closed Mediterranean forests, increasing abundance indicates an increase in fire frequency and burned areas, which are associated with more flammable vegetation under warmer and drier conditions. The same interpretation can be applied to samples off open Mediterranean woodland. However, the abundance should not be considered solely as an indicator of fire frequency and burned areas, as our study suggests that climate, fuel type, and flammability may also affect abundance. This methodology could improve the accuracy with which sedimentary charcoal records are interpreted.

We emphasize the need to calibrate the charcoal proxy in other ecosystems and over broader spatial scales to confirm its reliability. A high charcoal concentration has been previously associated with the occurrence of intense fires in the Iberian Peninsula Genet et al. (2021). However, upon extending the study area, it was observed that what had been designated as “intense fires” at the scale of the Iberian Peninsula corresponded to “low-intensity fires” at the scale of the western Mediterranean region.

6. Conclusion

Microscopic charcoal particles (measuring between 10 and 125 μm in length) were analysed in 277 marine surface sediment samples collected from the Iberian margin, the Gulf of Cadiz, and the western Mediterranean Sea. Microscopic charcoal concentration and morphology (elongation) were quantified and compared with fire regime characteristics (frequency, size and intensity), derived from remote sensing data, as well as climate and vegetation data, to better understand their spatial distribution in marine environments and help refine the interpretation of marine paleofire records.

The results show that relative changes in the mean length-to-width ratio of microscopic charcoal is a robust proxy for separating surface fires spreading in grass (elongated particles) versus crown forest fires (squared particles). In addition, an elongation ratio threshold of $<1.8 \pm 0.1$ seems to be a general indicator of tree combustion in marine paleo-fire records. The interpretation of variations in microscopic charcoal abundance is more complex. Within the same type of ecosystems, increasing abundance of microscopic charcoal indicates an increase in fire frequency and burned areas, associated with increasing flammability under a warmer and drier climate. However, in open vegetation (open mosaic vegetation) variations in abundance might also indicate a change in climate or a change in fuel type. This suggests that vegetation combustibility and flammability play also a role in controlling charcoal in marine sediments.

CRediT authorship contribution statement

Marion Genet: Conceptualization, Data curation, Formal analysis, Methodology, Writing – original draft, Writing – review & editing. **Anne-Laure Daniau:** Conceptualization, Investigation, Resources, Writing – original draft, Writing – review & editing. **Florent Mouillot:** Methodology, Resources, Writing – original draft. **Sabine Schmidt:** Methodology, Resources, Writing – review & editing. **Bernard Dennielou:** Funding acquisition, Writing – review & editing. **Serge Berné:** Writing – review & editing. **Vincent Hanquiez:** Writing – review & editing. **Mostefa E. Kouachi:** Writing – review & editing. **Muriel Georget:** Data curation, Methodology.

Declaration of competing interest

The authors declare that they have no known competing financial interests or personal relationships that could have appeared to influence the work reported in this paper.

Acknowledgement

This work was supported by the French INSU (Institut National des Sciences de l’Univers) programme LEFE (Les Enveloppes Fluides et l’Environnement) CAMPFIRE project; by theANR BRAISE project, grant ANR-19-CE01-0001-01 of the French Agence Nationale de la Recherche. M. Genet was supported by a doctoral fellowship from the University of Bordeaux. We thank Muriel Georget for laboratory assistance. We gratefully acknowledge I. Billy, O. Ther and L. Devaux for their technical help. We thank EPOC, LSCE and IFREMER laboratories for giving us access to their repositories of marine sediments. We thank IFREMER for access to sediment cores curated at CREAM (Centre de Resources en Echantillons et Archives Marins) seabed sediment and rock samples repository. Particular thanks go to the staff from Unite de Recherche G_eosciences Marines and from SISMER (French National Oceanographic Data Centre). The authors are grateful to the chief scientists, coring and logistic teams of the oceanographic cruises.

Appendix A. Supplementary data

Supplementary data to this article can be found online at https://doi.org/10.1016/j.qsa.2026.100333.

Data availability

Data will be made available on request.

References

Adolf, C., Wunderle, S., Colombaroli, D., Weber, H., Gobet, E., Heiri, O., Van Leeuwen, J. F.N., Bigler, C., Connor, S.E., Gałka, M., La Mantia, T., Makhortykh, S., Svitavská-Svobodová, H., Vannière, B., Tinner, W., 2018. The sedimentary and remote-sensing reflection of biomass burning in Europe. Global Ecol. Biogeogr. 27, 199–212. https://doi.org/10.1111/geb.12682.

Aleman, J.C., Blarquez, O., Bentaleb, I., Bonté, P., Brossier, B., Carcaillet, C., Gond, V., Gourlet-Fleury, S., Kpolita, A., Lefèvre, I., Oslisly, R., Power, M.J., Yongo, O., Bremond, L., Favier, C., 2013. Tracking land-cover changes with sedimentary charcoal in the Afrotropics. Holocene 23, 1853–1862. https://doi.org/10.1177/0959683613508159.

Alvarez, A., Gracia, M., Vayreda, J., Retana, J., 2012. Patterns of fuel types and crown fire potential in *Pinus halepensis* forests in the Western Mediterranean Basin. For. Ecol. Manag. 270, 282–290. https://doi.org/10.1016/j.foreco.2011.01.039.

Arfa, A.M.T., Benderradji, M.E.H., Alatou, D., 2009. Analyse des bilans des incendies de forêt et leur impact économique en Algérie entre 1985 et 2006 - [WWW Document]. https://newmedit.ciheam.org/edizioni_new_medit, 229,229,2009,85,246,analyse-des-bilans-des-incendies-de-for%C3%AAt-et-leur-impact-economique-en-algerie-entre-1985-et-2006.htm (accessed 11.20.25).

Arrogante-Funes, F., Mouillot, F., Moreira, B., Aguado, I., Chuvieco, E., 2024. Mapping and assessment of ecological vulnerability to wildfires in Europe. Fire Ecol. 20, 98. https://doi.org/10.1186/s42408-024-00321-8.

Bank, W., 2023. Note sur les Forêts Algériennes : gestion Durable des Forêts pour Lutter Contre les Feux de Forêts [WWW Document]. World Bank. URL. https://documents.

worldbank.org/en/publication/documents-reports/documentdetail/099110823163530127 (accessed 11.20.25).
Barbero, R., Curt, T., Ganteaume, A., Maillé, E., Jappiot, M., Bellet, A., 2019. Simulating the effects of weather and climate on large wildfires in France. Nat. Hazards Earth Syst. Sci. 19, 441–454. https://doi.org/10.5194/nhess-19-441-2019.
Barbosa, H.A., Buriti, C.O., Kumar, T.V.L., 2025. Assessment of fire dynamics in the amazon basin through satellite data. Atmosphere 16, 228. https://doi.org/10.3390/atmos16020228.
Batllori, E., Parisien, M., Krawchuk, M.A., Moritz, M.A., 2013. Climate change-induced shifts in fire for M editerranean ecosystems. Global Ecol. Biogeogr. 22, 1118–1129. https://doi.org/10.1111/geb.12065.
Beaufort, L., De Garidel-Thoron, T., Linsley, B., Oppo, D., Buchet, N., 2003. Biomass burning and oceanic primary production estimates in the Sulu Sea area over the last 380 kyr and the East Asian monsoon dynamics. Mar. Geol. 201, 53–65. https://doi.org/10.1016/S0025-3227(03)00208-1.
Belhadj-Khedher, C., El-Melki, T., Mouillot, F., 2020. Saharan hot and dry sirocco winds drive extreme fire events in Mediterranean Tunisia (North Africa). Atmosphere 11, 590. https://doi.org/10.3390/atmos11060590.
Belhadj-Khedher, C., Koutsias, N., Karamitsou, A., Ei-Melki, T., Ouelhazi, B., Hamdi, A., Nouri, H., Mouillot, F., 2018. A revised historical fire regime analysis in Tunisia (1985–2010) from a critical analysis of the national fire database and remote sensing. Forests 9, 59. https://doi.org/10.3390/f9020059.
Bowman, D.M.J.S., Balch, J.K., Artaxo, P., Bond, W.J., Carlson, J.M., Cochrane, M.A., D'Antonio, C.M., DeFries, R.S., Doyle, J.C., Harrison, S.P., Johnston, F.H., Keeley, J. E., Krawchuk, M.A., Kull, C.A., Marston, J.B., Moritz, M.A., Prentice, I.C., Roos, C.I., Scott, A.C., Swetnam, T.W., Van Der Werf, G.R., Pyne, S.J., 2009. Fire in the Earth system. Science 324, 481–484. https://doi.org/10.1126/science.1163886.
Bowring, S.P.K., Li, W., Mouillot, F., Rosan, T.M., Ciais, P., 2024. Road fragment edges enhance wildfire incidence and intensity, while suppressing global burned area. Nat. Commun. 15, 9176. https://doi.org/10.1038/s41467-024-53460-6.
Chergui, B., Fahd, S., Santos, X., Pausas, J.G., 2018. Socioeconomic factors drive fire-regime variability in the Mediterranean Basin. Ecosystems 21, 619–628. https://doi.org/10.1007/s10021-017-0172-6.
Chuvieco, E., Yebra, M., Martino, S., Thonicke, K., Gómez-Giménez, M., San-Miguel, J., Oom, D., Velea, R., Mouillot, F., Molina, J.R., Miranda, A.I., 2023. Towards an integrated approach to wildfire risk assessment: when, where, what and how may the landscapes burn. Fire 5 (5), 215.
Citing RStudio [WWW Document], 2025. Posit support. URL. https://support.posit.co/hc/en-us/articles/206212048-Citing-RStudio (accessed 6.17.25).
Crawford, A.J., Belcher, C.M., 2014. Charcoal morphometry for paleoecological analysis: the effects of fuel type and transportation on morphological parameters. Appl. Plant Sci. 2, 1400004. https://doi.org/10.3732/apps.1400004.
Curt, T., Aini, A., Dupire, S., 2020. Fire activity in mediterranean forests (The Algerian case). Fire 3, 58. https://doi.org/10.3390/fire3040058.
Daniau, A.-L., Desprat, S., Aleman, J.C., Bremond, L., Davis, B., Fletcher, W., Marlon, J. R., Marquer, L., Montade, V., Morales-Molino, C., Naughton, F., Rius, D., Urrego, D. H., 2019. Terrestrial plant microfossils in palaeoenvironmental studies, pollen, microcharcoal and phytolith. Towards a comprehensive understanding of vegetation, fire and climate changes over the past one million years. Rev. Micropaleontol. 63, 1–35. https://doi.org/10.1016/j.revmic.2019.02.001.
Daniau, A.-L., Goñi, M.F.S., Duprat, J., 2009. Last glacial fire regime variability in western France inferred from microcharcoal preserved in core MD04-2845, Bay of Biscay. Quat. Res. 71, 385–396. https://doi.org/10.1016/j.yqres.2009.01.007.
Daniau, A.-L., Loutre, M.-F., Swingedouw, D., Laepple, T., Bassinot, F., Malaizé, B., Kageyama, M., Charlier, K., Carfantan, H., 2023. Precession and obliquity forcing of the South African monsoon revealed by sub-tropical fires. Quat. Sci. Rev. 310, 108128. https://doi.org/10.1016/j.quascirev.2023.108128.
Daniau, A.-L., Sánchez-Goñi, M.F., Beaufort, L., Laggoun-Défarge, F., Loutre, M.-F., Duprat, J., 2007. Dansgaard–oeschger climatic variability revealed by fire emissions in southwestern Iberia. Quat. Sci. Rev. 26, 1369–1383. https://doi.org/10.1016/j.quascirev.2007.02.005.
Díaz-Delgado, R., Lloret, F., Pons, X., 2004. Statistical analysis of fire frequency models for Catalonia (NE Spain), 1975–1998) based on fire scar maps from Landsat MSS data. Int. J. Wildland Fire 13 (1), 89–99.
Dimitrakopoulos, A.P., 2002a. Mediterranean fuel models and potential fire behaviour in Greece. Int. J. Wildland Fire 11, 127–130. https://doi.org/10.1071/wf02018.
Dimitrakopoulos, A.P., 2002b. Mediterranean fuel models and potential fire behaviour in Greece. Int. J. Wildland Fire 11, 127–130. https://doi.org/10.1071/wf02018.
Dupont, L.M., Caley, T., Kim, J.-H., Castañeda, I., Malaizé, B., Giraudeau, J., 2011. Glacial-interglacial vegetation dynamics in South Eastern Africa coupled to sea surface temperature variations in the Western Indian Ocean. Clim. Past 7, 1209–1224. https://doi.org/10.5194/cp-7-1209-2011.
Dupont, L.M., Wyputta, U., 2003. Reconstructing pathways of aeolian pollen transport to the marine sediments along the coastline of SW Africa. Quat. Sci. Rev. 22, 157–174. https://doi.org/10.1016/S0277-3791(02)00032-X.
Fanget, A.-S., Bassetti, M.-A., Fontanier, C., Tudryn, A., Berné, S., 2016. Sedimentary archives of climate and sea-level changes during the Holocene in the Rhône prodelta (NW Mediterranean Sea). Clim. Past 12, 2161–2179. https://doi.org/10.5194/cp-12-2161-2016.
Fanget, A.-S., Berné, S., Jouet, G., Bassetti, M.-A., Dennielou, B., Maillet, G.M., Tondut, M., 2014. Impact of relative sea level and rapid climate changes on the architecture and lithofacies of the Holocene Rhone subaqueous delta (Western Mediterranean Sea). Sediment. Geol. 305, 35–53. https://doi.org/10.1016/j.sedgeo.2014.02.004.
Feurdean, A., 2021. Experimental production of charcoal morphologies to discriminate fuel source and fire type: an example from Siberian taiga. Biogeosciences 18, 3805–3821. https://doi.org/10.5194/bg-18-3805-2021.
Forkel, M., Dorigo, W., Lasslop, G., Chuvieco, E., Hantson, S., Heil, A., Teubner, I., Thonicke, K., Harrison, S.P., 2019. Recent global and regional trends in burned area and their compensating environmental controls. Environ. Res. Commun. 1, 051005. https://doi.org/10.1088/2515-7620/ab25d2.
Forrest, M., Hetzer, J., Billing, M., Bowring, S.P.K., Kosczor, E., Oberhagemann, L., Perkins, O., Warren, D., Arrogante-Funes, F., Thonicke, K., Hickler, T., 2024. Understanding and simulating cropland and non-cropland burning in Europe using the BASE (Burnt Area Simulator for Europe) model. Biogeosciences 21, 5539–5560. https://doi.org/10.5194/bg-21-5539-2024.
Fourcade, T., Sánchez Goñi, M.F., Lesven, J., Lahaye, C., Philippe, A., 2024. Vegetation response in NW Mediterranean borderlands to the millennial-scale climate variability of the last glacial period. Quat. Sci. Rev. 334, 108722. https://doi.org/10.1016/j.quascirev.2024.108722.
Fuchs, R., Herold, M., Verburg, P.H., Clevers, J.G.P.W., 2013. A high-resolution and harmonized model approach for reconstructing and analysing historic land changes in Europe. Biogeosciences 10, 1543–1559.
Ganteaume, A., Camia, A., Jappiot, M., San-Miguel-Ayanz, European Commission, 2013. A Review of the Main Driving Factors of Forest Fire Ignition over Europe. ResearchGate. https://doi.org/10.1007/s00267-012-9961-z.
Ganteaume, A., Lampin-Maillet, C., Guijarro, M., Hernando, C., Jappiot, M., Fonturbel, T., Perez-Gorostiaga, P., Vega, J.A., 2009. Spot fires: fuel bed flammability and capability of firebrands to ignite fuel beds. Int. J. Wildland Fire 18, 18. https://doi.org/10.1071/WF07111.
Genet, M., Daniau, A.-L., Mouillot, F., Hanquiez, V., Schmidt, S., David, V., Georget, M., Abrantes, F., Anschutz, P., Bassinot, F., Bonnin, J., Dennielou, B., Eynaud, F., Hodell, D.A., Mulder, T., Naughton, F., Rossignol, L., Tzedakis, P., Sánchez-Goñi, M. F., 2021. Modern relationships between microscopic charcoal in marine sediments and fire regimes on adjacent landmasses to refine the interpretation of marine paleofire records: an Iberian case study. Quat. Sci. Rev. 270, 107148. https://doi.org/10.1016/j.quascirev.2021.107148.
Genet, M., Daniau, A.-L., Mouillot, F., Leys, B., Bassetti, M.-A., Azuara, J., Jalali, B., Sicre, M.-A., Berné, S., Georget, M., 2025. Persistence of a wind-driven fire regime in Mediterranean France over the past 8200 years revealed by a marine paleoecological record. The Holocene 09596836251350236. https://doi.org/10.1177/09596836251350236.
Giglio, L., Boschetti, L., Roy, D.P., Humber, M.L., Justice, C.O., 2018. The Collection 6 MODIS burned area mapping algorithm and product. Rem. Sens. Environ. 217, 72–85. https://doi.org/10.1016/j.rse.2018.08.005.
Giglio, L., Schroeder, W., Justice, C.O., 2016. The collection 6 MODIS active fire detection algorithm and fire products. Rem. Sens. Environ. 178, 31–41. https://doi.org/10.1016/j.rse.2016.02.054.
Gincheva, A., Pausas, J.G., Edwards, A., 2024. A Monthly Gridded Burned Area Database of National Wildland Fire Data. Scientific Data [WWW Document]. URL. https://www.nature.com/articles/s41597-024-03141-2 (accessed 11.20.25).
Grünig, M., Seidl, R., Senf, C., 2023. Increasing aridity causes larger and more severe forest fires across Europe. Glob. Change Biol. 29, 1648–1659. https://doi.org/10.1111/gcb.16547.
Haas, O., Prentice, I.C., Harrison, S.P., 2022. Global environmental controls on wildfire burnt area, size, and intensity. Environ. Res. Lett. 17, 065004. https://doi.org/10.1088/1748-9326/ac6a69.
Haliuc, A., Daniau, A.-L., Mouillot, F., Chen, W., Leys, B., David, V., Hanquiez, V., Dennielou, B., Schefuß, E., Bayon, G., Crosta, X., 2023a. Microscopic charcoals in ocean sediments off Africa track past fire intensity from the continent. Commun. Earth Environ. 4, 133. https://doi.org/10.1038/s43247-023-00800-x.
Haliuc, A., Daniau, A.-L., Mouillot, F., Chen, W., Leys, B., David, V., Hanquiez, V., Dennielou, B., Schefuß, E., Bayon, G., Crosta, X., 2023b. Microscopic charcoals in ocean sediments off Africa track past fire intensity from the continent. Commun. Earth Environ. 4, 133. https://doi.org/10.1038/s43247-023-00800-x.
Hantson, S., Arneth, A., Harrison, S.P., Kelley, D.I., Prentice, I.C., Rabin, S.S., Archibald, S., Mouillot, F., Arnold, S.R., Artaxo, P., Bachelet, D., Ciais, P., Forrest, M., Friedlingstein, P., Hickler, T., Kaplan, J.O., Kloster, S., Knorr, W., Lasslop, G., Li, F., Mangeon, S., Melton, J.R., Meyn, A., Sitch, S., Spessa, A., van der Werf, G.R., Voulgarakis, A., Yue, C., 2016. The status and challenge of global fire modelling. Biogeosciences 13, 3359–3375. https://doi.org/10.5194/bg-13-3359-2016.
Harper, K.L., Lamarche, C., Hartley, A., Peylin, P., Ottlé, C., Bastrikov, V., San Martín, R., Bohnenstengel, S.I., Kirches, G., Boettcher, M., Shevchuk, R., Brockmann, C., Defourny, P., 2023. A 29-year time series of annual 300 m resolution plant-functional-type maps for climate models. Earth Syst. Sci. Data (15), 1465–1499. https://doi.org/10.5194/essd-15-1465-2023.
Heusser, L.E., 1983. Pollen distribution in the bottom sediments of the western North Atlantic Ocean. Mar. Micropaleontol. 8, 77–88. https://doi.org/10.1016/0377-8398(83)90006-3.
Heusser, L., Balsam, W.L., 1977. Pollen distribution in the Northeast Pacific Ocean. Quat. Res. 7, 45–62. https://doi.org/10.1016/0033-5894(77)90013-8.
Hooghiemstra, H., Lézine, A.-M., Leroy, S.A.G., Dupont, L., Marret, F., 2006. Late Quaternary palynology in marine sediments: a synthesis of the understanding of pollen distribution patterns in the NW African setting. Quat. Int. 148, 29–44. https://doi.org/10.1016/j.quaint.2005.11.005.
Inoue, J., Usuki, T., n.d. Effects of particle size and pretreatment methods on the morphometry of grass charcoal particles: implications for morphometric analysis of microcharcoal particles - Jun Inoue, Tatsuya Usuki, 2025 [WWW Document]. URL

https://journals.sagepub.com/doi/abs/10.1177/09596836241307296 (accessed 10.2.25).
Joannin, S., Brugiapaglia, E., de Beaulieu, J.-L., Bernardo, L., Magny, M., Peyron, O., Goring, S., Vannière, B., 2012. Pollen-based reconstruction of Holocene vegetation and climate in southern Italy: the case of Lago Trifoglietti. Clim. Past 8, 1973–1996. https://doi.org/10.5194/cp-8-1973-2012.
Kassambara, A., Mundt, F., 2020. factoextra: Extract and Visualize the Results of Multivariate Data Analyses.
Keeley, J.E., Bond, W.J., Bradstock, R.A., Pausas, J.G., Rundel, P.W., 2011a. Fire in Mediterranean Ecosystems: Ecology, Evolution and Management. Cambridge University Press.
Keeley, J.E., Pausas, J.G., Rundel, P.W., Bond, W.J., Bradstock, R.A., 2011b. Fire as an evolutionary pressure shaping plant traits. Trends Plant Sci. 16, 406–411. https://doi.org/10.1016/j.tplants.2011.04.002.
Kloster, S., Mahowald, N.M., Randerson, J.T., Thornton, P.E., Hoffman, F.M., Levis, S., Lawrence, P.J., Feddema, J.J., Oleson, K.W., Lawrence, D.M., 2010. Fire dynamics during the 20th century simulated by the Community Land Model. Biogeosciences 7, 1877–1902. https://doi.org/10.5194/bg-7-1877-2010.
Kolde, R., 2025. Pheatmap: Pretty Heatmaps.
Kouachi, M.E., Khairoun, A., Moghli, A., Rahmani, S., Mouillot, F., Baeza, M.J., Moutahir, H., 2024. Forty-year fire history reconstruction from landsat data in mediterranean ecosystems of Algeria following international standards. Remote Sens. 16, 2500. https://doi.org/10.3390/rs16132500.
Krawchuk, M.A., Moritz, M.A., 2011. Constraints on global fire activity vary across a resource gradient. Ecology 92, 121–132. https://doi.org/10.1890/09-1843.1.
Krebs, P., Pezzatti, G.B., Mazzoleni, S., Talbot, L.M., Conedera, M., 2010. Fire regime: history and definition of a key concept in disturbance ecology. Theory Biosci. 129, 53–69. https://doi.org/10.1007/s12064-010-0082-z.
Lê, S., Josse, J., Husson, F., 2008. FactoMineR: an R package for multivariate analysis. J. Stat. Software 25, 1–18. https://doi.org/10.18637/jss.v025.i01.
Lambert, C., Penaud, A., Vidal, M., Gandini, C., Labeyrie, L., Chauvaud, L., Ehrhold, A., 2020. Striking forest revival at the end of the Roman Period in north-western Europe. Sci. Rep. 10, 21984. https://doi.org/10.1038/s41598-020-77253-1.
Laurent, P., Mouillot, F., Yue, C., Ciais, P., Moreno, M.V., Nogueira, J.M.P., 2018. FRY, a global database of fire patch functional traits derived from space-borne burned area products. Sci. Data 5, 180132. https://doi.org/10.1038/sdata.2018.132.
Lecina-Diaz, J., Martínez-Vilalta, J., Alvarez, A., Vayreda, J., Retana, J., 2021. Assessing the risk of losing forest ecosystem services due to wildfires. Ecosystems 24, 1687–1701. https://doi.org/10.1007/s10021-021-00611-1.
Leys, B., Brewer, S.C., McConaghy, S., Mueller, J., McLauchlan, K.K., 2015. Fire history reconstruction in grassland ecosystems: amount of charcoal reflects local area burned. Environ. Res. Lett. 10, 114009. https://doi.org/10.1088/1748-9326/10/11/114009.
Loepfe, L., Rodrigo, A., Lloret, F., 2014. Two thresholds determine climatic control of forest fire size in Europe and northern Africa. Reg. Environ. Change 14, 1395–1404. https://doi.org/10.1007/s10113-013-0583-7.
Madoui, A., 2002. Les incendies de forêt en Algérie. Historique, bilan et analyse. Forêt Méditerranéenne XXIII, 23–30.
Majdalani, G., Koutsias, N., Faour, G., Adjizian-Gerard, J., Mouillot, F., 2022. Fire regime analysis in Lebanon (2001–2020): combining remote sensing data in a scarcely documented area. Fire 5, 141. https://doi.org/10.3390/fire5050141.
Marlon, J., Bartlein, P.J., Whitlock, C., 2006. Fire-fuel-climate linkages in the northwestern USA during the Holocene. Holocene 16, 1059–1071. https://doi.org/10.1177/0959683606069396.
Marlon, J.R., Kelly, R., Daniau, A.-L., Vannière, B., Power, M.J., Bartlein, P., Higuera, P., Blarquez, O., Brewer, S., Brücher, T., Feurdean, A., Gil-Romera, G., Iglesias, V., Maezumi, S.Y., Magi, B., Mustaphi, C.J.C., Zhihai, T., 2015. Reconstructions of biomass burning from sediment charcoal records to improve data-model comparisons. https://doi.org/10.5194/bgd-12-18571-2015.
Marquer, L., Gaillard, M.-J., Sugita, S., Trondman, A.-K., Mazier, F., Nielsen, A.B., Fyfe, R.M., Odgaard, B.V., Alenius, T., Birks, H.J.B., Bjune, A.E., Christiansen, J., Dodson, J., Edwards, K.J., Giesecke, T., Herzschuh, U., Kangur, M., Lorenz, S., Poska, A., Schult, M., Seppä, H., 2014. Holocene changes in vegetation composition in northern Europe: why quantitative pollen-based vegetation reconstructions matter. Quat. Sci. Rev. 90, 199–216. https://doi.org/10.1016/j.quascirev.2014.02.013.
McNorton, J., 2025. Global data-driven prediction of fire activity. https://doi.org/10.5194/egusphere-egu25-17607.
Meddour-Sahar, O., 2015. Wildfires in Algeria: problems and challenges. iForest 8, 818–826. https://doi.org/10.3832/ifor1279-007.
Meddour-Sahar, O., Meddour, R., Arezki, D., 2008. Les Feux De Forêts En Algérie Sur Le Temps Long (1876-2007) [WWW Document]. ResearchGate. URL. https://www.researchgate.net/publication/288910102_Les_feux_de_forets_en_Algerie_sur_le_temps_long_1876-2007 (accessed 11.20.25).
Meddour-Sahar, O., Meddour, R., Leone, V., Lovreglio, R., Derridj, A., 2013. Analysis of forest fires causes and their motivations in northern Algeria: the Delphi method. iFor. Biogeosci. For. 6, 247. https://doi.org/10.3832/ifor0098-006.
Meddour-Sahar, Ouahiba, Lovreglio, R., Meddour, R., Leone, V., Derridj, A., 2013. Fire and people in three rural communities in Kabylia (Algeria): results of a survey. Open J. For. 3, 30–40. https://doi.org/10.4236/ojf.2013.31006.
Mensing, S.A., Michaelsen, J., Byrne, R., 1999. A 560-Year record of Santa Ana fires reconstructed from charcoal deposited in the Santa Barbara Basin, California. Quat. Res. 51, 295–305. https://doi.org/10.1006/qres.1999.2035.
Müller, P.J., Kirst, G., Ruhland, G., von Storch, I., Rosell-Melé, A., 1998. Calibration of the alkenone paleotemperature index U37K′ based on core-tops from the eastern South Atlantic and the global ocean (60°N-60°S). Geochem. Cosmochim. Acta 62, 1757–1772. https://doi.org/10.1016/S0016-7037(98)00097-0.
Morales-Molino, C., Devaux, L., Georget, M., Hanquiez, V., Sánchez Goñi, M.F., 2020. Modern pollen representation of the vegetation of the Tagus Basin (central Iberian Peninsula). Rev. Palaeobot. Palynol. 276, 104193. https://doi.org/10.1016/j.revpalbo.2020.104193.
Moreno, J.M., Morales-Molino, C., Torres, I., Arianoutsou, M., 2021. Fire in mediterranean pine forests: past, present and future. In: Ne'eman, G., Osem, Y. (Eds.), Pines and their Mixed Forest Ecosystems in the Mediterranean Basin, Managing Forest Ecosystems. Springer International Publishing, Cham, pp. 421–456. https://doi.org/10.1007/978-3-030-63625-8_21.
Moriondo, M., Good, P., Durao, R., Bindi, M., Giannakopoulos, C., Corte-Real, J., 2006. Potential impact of climate change on fire risk in the Mediterranean area. Clim. Res. 31, 85–95. https://doi.org/10.3354/cr031085.
Mouillot, F., Rambal, S., Joffre, R., 2002. Simulating climate change impacts on fire frequency and vegetation dynamics in a Mediterranean-type ecosystem. Glob. Change Biol. 8, 423–437. https://doi.org/10.1046/j.1365-2486.2002.00494.x.
Mouillot, F., Schultz, M.G., Yue, C., Cadule, P., Tansey, K., Ciais, P., Chuvieco, E., 2014. Ten years of global burned area products from spaceborne remote sensing—A review: analysis of user needs and recommendations for future developments. Int. J. Appl. Earth Obs. Geoinf. 26, 64–79. https://doi.org/10.1016/j.jag.2013.05.014.
Mouillot, F., Field, C.B., 2005. Fire history and the global carbon budget: a 1°× 1° fire history reconstruction for the 20th century. Glob. Change Biol. 11, 398–420. https://doi.org/10.1111/j.1365-2486.2005.00920.x.
Mudie, P.J., 1982. Pollen distribution in recent marine sediments, eastern Canada. Can. J. Earth Sci. 19, 729–747. https://doi.org/10.1139/e82-062.
Naughton, F., Sánchez Goñi, M.F., Drago, T., Conceição Freitas, M., Oliveira, A., 2007. Holocene changes in the douro Estuary (Northwestern iberia). J. Coast Res. 23, 711–720. https://doi.org/10.2112/05-0462.1.
New, M., Lister, D., Hulme, M., Makin, I., 2002. A high-resolution data set of surface climate over global land areas. Clim. Res. 21, 1–25. https://doi.org/10.3354/cr021001.
Nichols, G.J., Cripps, J.A., Collinson, M.E., Scott, A.C., 2000. Experiments in waterlogging and sedimentology of charcoal: results and implications. Palaeogeography, Palaeoclimatology, Palaeoecology, Fire and the Palaeoenvironment 164, 43–56. https://doi.org/10.1016/S0031-0182(00)00174-7.
Olson, D.M., Dinerstein, E., Wikramanayake, E.D., Burgess, N.D., Powell, G.V.N., Underwood, E.C., D'amico, J.A., Itoua, I., Strand, H.E., Morrison, J.C., Loucks, C.J., Allnutt, T.F., Ricketts, T.H., Kura, Y., Lamoreux, J.F., Wettengel, W.W., Hedao, P., Kassem, K.R., 2001. Terrestrial ecoregions of the world: a new map of life on Earth: a new global map of terrestrial ecoregions provides an innovative tool for conserving biodiversity. Bioscience 51 (2), 933–938. https://doi.org/10.1641/0006-3568(2001)051%255B0933:TEOTWA%255D2.0.CO.
Patterson, W.A., Edwards, K.J., Maguire, D.J., 1987. Microscopic charcoal as a fossil indicator of fire. Quat. Sci. Rev. 6, 3–23. https://doi.org/10.1016/0277-3791(87)90012-6.
Pausas, J.G., 1999. Response of plant functional types to changes in the fire regime in Mediterranean ecosystems: a simulation approach. J. Veg. Sci. 10, 717–722. https://doi.org/10.2307/3237086.
Pausas, J.G., 2004. Changes in fire and climate in the eastern iberian peninsula (Mediterranean Basin). Clim. Change 63, 337–350. https://doi.org/10.1023/B:CLIM.0000018508.94901.9c.
Pausas, J.G., Keeley, J.E., Schwilk, D.W., 2017. Flammability as an ecological and evolutionary driver. J. Ecol. 105, 289–297. https://doi.org/10.1111/1365-2745.12691.
Pausas, J.G., Paula, S., 2012a. Fuel shapes the fire–climate relationship: evidence from Mediterranean ecosystems. Global Ecol. Biogeogr. 21, 1074–1082. https://doi.org/10.1111/j.1466-8238.2012.00769.x.
Pausas, J.G., Paula, S., 2012b. Fuel shapes the fire–climate relationship: evidence from Mediterranean ecosystems. Global Ecol. Biogeogr. 21, 1074–1082. https://doi.org/10.1111/j.1466-8238.2012.00769.x.
Pereboom, E.M., Vachula, R.S., Huang, Y., Russell, J., 2020. The morphology of experimentally produced charcoal distinguishes fuel types in the Arctic tundra. Holocene 30, 1091–1096. https://doi.org/10.1177/0959683620908629.
Poulter, B., MacBean, N., Hartley, A., Khlystova, I., Arino, O., Betts, R., Bontemps, S., Boettcher, M., Brockmann, C., Defourny, P., Hagemann, S., Herold, M., Kirches, G., Lamarche, C., Lederer, D., Ottlé, C., Peters, M., Peylin, P., 2015. Plant functional type classification for earth system models: results from the European space Agency's land cover climate change initiative. Geosci. Model Dev. 8, 2315–2328. https://doi.org/10.5194/gmd-8-2315-2015.
Pugnet, L., Lourenço, L., Rocha, J., 2010. L'ignition des feux de forêt par l'action de la foudre au Portugal de 1996 à 2008. Territorium 57–70. https://doi.org/10.14195/1647-7723_17_6.
Rabin, S.S., Melton, J.R., Lasslop, G., Bachelet, D., Forrest, M., Hantson, S., Kaplan, J.O., Li, F., Mangeon, S., Ward, D.S., Yue, C., Arora, V.K., Hickler, T., Kloster, S., Knorr, W., Nieradzik, L., Spessa, A., Folberth, G.A., Sheehan, T., Voulgarakis, A., Kelley, D.I., Prentice, I.C., Sitch, S., Harrison, S., Arneth, A., 2017. The fire modeling intercomparison project (FireMIP), phase 1: experimental and analytical protocols with detailed model descriptions. Geosci. Model Dev. 10, 1175–1197. https://doi.org/10.5194/gmd-10-1175-2017.
Ruffault, J., Curt, T., Moron, V., Trigo, R.M., Mouillot, F., Koutsias, N., Pimont, F., Martin-StPaul, N., Barbero, R., Dupuy, J.-L., Russo, A., Belhadj-Khedher, C., 2020. Increased likelihood of heat-induced large wildfires in the Mediterranean Basin. Sci. Rep. 10, 13790. https://doi.org/10.1038/s41598-020-70069-z.

Ruffault, J., Mouillot, F., 2015. How a new fire-suppression policy can abruptly reshape the fire-weather relationship. Ecosphere 6. https://doi.org/10.1890/ES15-00182.1 art199.

Ruiz, F., Lopez, G., 2010. Review of Cultivation, History and Uses of Eucalypts in Spain.

San-Miguel-Ayanz, J., Durrant, T., Boca, R., Maianti, P., Liberta, G., Jacome, F.O., Branco, A., De, R., Suarez-Moreno, M., Ferrari, D., 2023. Forest Fires in Europe, Middle East and North Africa 2022.

Sayedi, S.S., Abbott, B.W., Vannière, B., Leys, B., Colombaroli, D., Romera, G.G., Słowiński, M., Aleman, J.C., Blarquez, O., Feurdean, A., Brown, K., Aakala, T., Alenius, T., Allen, K., Andric, M., Bergeron, Y., Biagioni, S., Bradshaw, R., Bremond, L., Brisset, E., Brooks, J., Brugger, S.O., Brussel, T., Cadd, H., Cagliero, E., Carcaillet, C., Carter, V., Catry, F.X., Champreux, A., Chaste, E., Chavardès, R.D., Chipman, M., Conedera, M., Connor, S., Constantine, M., Courtney Mustaphi, C., Dabengwa, A.N., Daniels, W., De Boer, E., Dietze, E., Estrany, J., Fernandes, P., Finsinger, W., Flantua, S.G.A., Fox-Hughes, P., Gaboriau, D.M., Gayo, M., Girardin, E., Martin, P., Glenn, J., Glückler, R., González-Arango, C., Groves, M., Hamilton, D.S., Hamilton, R.J., Hantson, S., Hapsari, K.A., Hardiman, M., Hawthorne, D., Hoffman, K., Inoue, J., Karp, A.T., Krebs, P., Kulkarni, C., Kuosmanen, N., Lacourse, T., Ledru, M.-P., Lestienne, M., Long, C., López-Sáez, J.A., Loughlin, N., Niklasson, M., Madrigal, J., Maezumi, S.Y., Marcisz, K., Mariani, M., McWethy, D., Meyer, G., Molinari, C., Montoya, E., Mooney, S., Morales-Molino, C., Morris, J., Moss, P., Oliveras, I., Pereira, J.M., Pezzatti, G.B., Pickarski, N., Pini, R., Rehn, E., Remy, C.C., Revelles, J., Rius, D., Robin, V., Ruan, Y., Rudaya, N., Russell-Smith, J., Seppä, H., Shumilovskikh, L., Sommers, W.T., Tavşanoğlu, Ç., Umbanhowar, C., Urquiaga, E., Urrego, D., Vachula, R.S., Wallenius, T., You, C., Daniau, A.-L., 2024. Assessing changes in global fire regimes. Fire Ecol. 20, 18. https://doi.org/10.1186/s42408-023-00237-9.

Sicre, M.-A., Jalali, B., Martrat, B., Schmidt, S., Bassetti, M.-A., Kallel, N., 2016. Sea surface temperature variability in the North Western Mediterranean Sea (Gulf of Lion) during the common era. Earth Planet Sci. Lett. 456, 124–133. https://doi.org/10.1016/j.epsl.2016.09.032.

Turco, M., Rosa-Cánovas, J.J., Bedia, J., Jerez, S., Montávez, J.P., Llasat, M.C., Provenzale, A., 2018. Exacerbated fires in Mediterranean Europe due to anthropogenic warming projected with non-stationary climate-fire models. Nat. Commun. 9, 3821. https://doi.org/10.1038/s41467-018-06358-z.

UmbanhowarJr, C.E., Mcgrath, M.J., 1998. Experimental production and analysis of microscopic charcoal from wood, leaves and grasses. Holocene 8, 341–346. https://doi.org/10.1191/095968398666496051.

Vachula, R.S., Rehn, E., 2023. Modeled dispersal patterns for wood and grass charcoal are different: implications for paleofire reconstruction. Holocene 33, 159–166. https://doi.org/10.1177/09596836221131708.

Van der Meersch, V., Armstrong, E., Mouillot, F., Duputié, A., Davi, H., Saltré, F., Chuine, I., 2025. Paleorecords reveal biological mechanisms crucial for reliable species range shift projections amid rapid climate change. Ecol. Lett. 28, e70080. https://doi.org/10.1111/ele.70080.

Whitlock, C., Larsen, C., 2001. Charcoal as a fire proxy. In: Smol, J.P., Birks, H.J.B., Last, W.M., Bradley, R.S., Alverson, K. (Eds.), Tracking Environmental Change Using Lake Sediments: Terrestrial, Algal, and Siliceous Indicators. Springer, Netherlands, Dordrecht, pp. 75–97. https://doi.org/10.1007/0-306-47668-1_5.

Wickham, H., Averick, M., Bryan, J., Chang, W., McGowan, L., François, R., Grolemund, G., Hayes, A., Henry, L., Hester, J., Kuhn, M., Pedersen, T., Miller, E., Bache, S., Müller, K., Ooms, J., Robinson, D., Seidel, D., Spinu, V., Takahashi, K., Vaughan, D., Wilke, C., Woo, K., Yutani, H., 2019. Welcome to the tidyverse. JOSS 4, 1686. https://doi.org/10.21105/joss.01686.

Yue, C., Ciais, P., Cadule, P., Thonicke, K., van Leeuwen, T.T., 2015. Modelling the role of fires in the terrestrial carbon balance by incorporating SPITFIRE into the global vegetation model ORCHIDEE – part 2: carbon emissions and the role of fires in the global carbon balance. Geosci. Model Dev. 8, 1321–1338. https://doi.org/10.5194/gmd-8-1321-2015.

Zanon, M., Davis, B.A.S., Marquer, L., Brewer, S., Kaplan, J.O., 2018. European Forest cover during the past 12,000 years: a palynological reconstruction based on modern analogs and remote sensing. Front. Plant Sci. 9, 253. https://doi.org/10.3389/fpls.2018.00253.

Zhang, L., Mo, L., Fan, C., Zhou, H., Zhao, Y., 2023. Data-driven prediction methods for real-time indoor fire scenario inferences. Fire 6, 401. https://doi.org/10.3390/fire6100401.

Zhao, X., Kaniewski, D., Wang, Y., Marriner, N., Salem, A., Liu, Y., Chen, J., Sun, Q., Finlayson, B., Otto, T., Luce, F., Chen, Z., 2025. Holocene trends in Nile Delta fire regimes driven by cropland expansion and reduced precipitation. Quat. Sci. Rev. 361, 109412. https://doi.org/10.1016/j.quascirev.2025.109412.